R. & M. No. 3098
(19,633)
A.R.C. Technical Report

MINISTRY OF SUPPLY

AERONAUTICAL RESEARCH COUNCIL
REPORTS AND MEMORANDA

The Shape of the Centre Part of a Swept-Back Wing with a Required Load Distribution

By

J. WEBER, Dr. rer. nat.

LONDON: HER MAJESTY'S STATIONERY OFFICE
1959
TWELVE SHILLINGS NET

The Shape of the Centre Part of a Swept-Back Wing with a Required Load Distribution

By

J. WEBER, Dr.rer.nat.

COMMUNICATED BY THE DIRECTOR-GENERAL OF SCIENTIFIC RESEARCH (AIR), MINISTRY OF SUPPLY

Reports and Memoranda No. 3098*

May, 1957

Summary.—A method is developed for designing the centre portion of a cambered and twisted swept-back wing to have the same chordwise load distribution at all spanwise stations. For this purpose the downwash field induced by a doublet distribution of constant spanwise strength in the chordal plane of a constant-chord wing is determined for incompressible, sonic and supersonic main-stream flow. Since the downwash has a logarithmic singularity at the centre section in the chordal plane itself, an approximate method is suggested to satisfy the boundary condition at the surface of the thick wing. Numerical examples illustrate the influence of the angle of sweep, the wing thickness and the load distribution. They show in particular that the required shape does not vary much with Mach number. A relatively rapid change of twist and camber with the spanwise distance from the centre section is required as shown by calculated results for sonic flow. There is some reason for using the camber and twist designed for the centre section of the isolated wing also for wing-fuselage junctions.

1. *Introduction.*—This note deals with the problem of determining the shape of a lifting swept-back wing with a given spanwise and chordwise load distribution. It is known that the flow in the centre region of a swept wing is highly three-dimensional and therefore differs considerably from that on a two-dimensional wing, which implies that the section shape (camber and twist) at the centre of the wing must differ from that at stations away from the centre if a given chordwise load distribution is required everywhere. It is the aim of this note to determine the camber and twist at the centre part of a swept-back wing when the load distribution is given. The design of such a wing with a load distribution which is constant along lines parallel to the leading edge is of practical interest since, together with a properly chosen thickness distribution, such a wing may have straight and fully swept isobars, whereas otherwise the benefit of sweep is largely lost over the central part of the wing.

With this type of load distribution, a mathematical difficulty arises if linear theory is applied in its standard form such that the boundary condition (of zero normal velocity at the wing surface) is satisfied in the chordal plane instead of at the wing surface. Constant spanwise load distributions lead to a singular behaviour of the downwash induced at the centre-line of the wing as can easily be seen in the case of subsonic flow where the load distribution under consideration can be represented by straight vortex lines which have a kink at the centre section. This implies that, in the present case, we cannot calculate the induced velocities at the position of the singularities and add the velocity increments due to the thickness distribution of the wing afterwards. We must take account of the wing thickness and of the load distribution simultaneously and satisfy the boundary condition at the surface of the thick cambered wing.

*R.A.E. Report Aero. 2591, received 5th November, 1957.

An approximation to the correct procedure is obtained by calculating the downwash induced by a plane sheet of vortices or doublets at points which are displaced from the sheet by half the local wing thickness. Though we depart in this respect from the usual linear theory, we still make the assumption that thickness, camber and twist are small so that it is justified to use the linearized potential equation.

The flow at subsonic, sonic and low supersonic speeds is considered to study the effect of the free-stream Mach number. To isolate the centre effect in incompressible flow we consider only wings of infinite span (*i.e.*, constant chord), which implies the absence of trailing vortices. A restriction to infinite wings is, of course, not necessary with sonic or supersonic main flow. In the case of a supersonic main stream, only wings with subsonic leading edges are treated.

The downwash field which is induced at the centre section by a plane sheet of doublets with constant strength along the span is calculated in Section 2 for a supersonic main stream, in Section 3 for sonic main stream and in Section 4 for incompressible flow. In Section 5, the assumptions inherent in the approximate method for calculating the normal velocity induced at the surface of the thick cambered and twisted wing are discussed. Some numerical examples are given in Section 6 to illustrate the effect of the free-stream Mach number, of the chordwise load distribution chosen, and of the wing thickness and the angle of sweep. The variation of the section shape with spanwise distance from the centre section is calculated in Section 7 for sonic main flow. In Section 8, it is shown that a similar singular behaviour of the downwash occurs in the junction of a fuselage and a swept wing as in the centre section of the isolated wing. A few load distributions which avoid the singular behaviour of the downwash are considered in Section 9.

2. *The Downwash Induced in Supersonic Flow.*—2.1. *General Relations.*—Let x, y, z be a right-handed system of Cartesian co-ordinates with the origin at the leading edge of the centre section, the x axis taken in the direction of the undisturbed stream and y spanwise. The wing chord c at the centre section of the wing is taken as unity throughout. The undisturbed stream has a velocity V_0 and a Mach number M_0, and $\beta = \sqrt{(M_0^2 - 1)}$.

Our aim is to determine the shape $z(x, y)$ of a wing of given plan-form and given load distribution. The wing surface is a stream surface which can be calculated if the velocity field is known. In this note, the linearised boundary condition

$$\frac{\partial z(x, y)}{\partial x} = \frac{v_z(x, y, z)}{V_0} \qquad \ldots \ldots \ldots \ldots \ldots \ldots \ldots \ldots \qquad (1)$$

will be used to determine the wing shape (*see* Section 5). The downwash v_z can be calculated by determining first the perturbation velocity potential ϕ which satisfies the equation of motion and satisfies the boundary condition at the wing imposed by the given load distribution. The velocity component v_z is then determined by differentiation with respect to z.

With a surface doublet distribution in the plane $z = 0$ and supersonic main stream the perturbation velocity potential ϕ, which satisfies the linear potential equation, is determined as the ' finite part ' of (*see, e.g.*, Ref. 1, p. 445) :

$$\phi(x, y, z) = -\frac{\beta^2 z}{2\pi} \int\int \frac{\phi_U(x', y') - \phi_L(x', y')}{\sqrt{\{(x - x')^2 - \beta^2(y - y')^2 - \beta^2 z^2\}^3}}\, dx'\, dy' , \qquad \ldots \ldots \qquad (2)$$

where the integration has to be carried out over the part of the doublet distribution lying within the Mach fore-cone from the point x, y, z :

$$(x - x')^2 > \beta^2(y - y')^2 + \beta^2 z^2$$
$$x > x'.$$

The suffices $_U$ and $_L$ denote the upper and lower surfaces of the wing, *i.e.*, of the doublet distribution. We introduce the load coefficient $l(x, y)$:

$$
\begin{aligned}
l(x, y) &= -\Delta C_p(x, y) \\
&= -\{C_{pU}(x, y) - C_{pL}(x, y)\} \\
&= 2\left\{\frac{v_{xU}(x, y)}{V_0} - \frac{v_{xL}(x, y)}{V_0}\right\} \\
&= \frac{2}{V_0}\left\{\frac{\partial \phi_U(x, y)}{\partial x} - \frac{\partial \phi_L(x, y)}{\partial x}\right\} \quad \ldots \quad (3)
\end{aligned}
$$

Integrating equation (2) by parts with respect to x' and taking the ' finite part ' we obtain for a wing with subsonic leading edges the equation :

$$
\phi(x, y, z) = \frac{zV_0}{4\pi}\int\int \frac{l(x', y')(x - x')}{\{(y - y')^2 + z^2\}\sqrt{[(x - x')^2 - \beta^2\{(y - y')^2 + z^2\}]}}\, dx'\, dy' \ldots \quad (4)
$$

Thus, for given load distribution $l(x, y)$, the potential ϕ can be determined by integration. Differentiation with respect to z gives the downwash v_z and by another integration (equation (1)), the shape of the stream surface, *i.e.*, the required shape of the aerofoil, is obtained.

We deal in this section only with the centre section of the wing. For this :

$$
\phi(x, o, z) = \frac{zV_0}{2\pi}\int\int \frac{l(x', y')(x - x')}{(y'^2 + z^2)\sqrt{\{(x - x')^2 - \beta^2 y'^2 - \beta^2 z^2)\}}}\, dx'\, dy'. \quad \ldots \quad (5)
$$

The integral is to be taken over the part of the wing for which $y' > 0$ and $x - x' > \beta\sqrt{(y'^2 + z^2)}$. Therefore

$$
\begin{aligned}
\phi(x, o, z) = \frac{V_0}{2\pi}\int_0^{x_1} z(x - x') \int_0^{x'/\tan\varphi} \frac{l(x', y')\, dy'}{(y'^2 + z^2)\sqrt{\{(x - x')^2 - \beta^2 y'^2 - \beta^2 z^2\}}}\, dx' \\
+ \frac{V_0}{2\pi}\int_{x_1}^{x - \beta z} z(x - x') \int_0^{(1/\beta)\sqrt{\{(x - x')^2 - \beta^2 z^2\}}} \frac{l(x', y')\, dy'}{(y'^2 + z^2)\sqrt{\{(x - x')^2 - \beta^2 y'^2 - \beta^2 z^2\}}}\, dx', \quad (6)
\end{aligned}
$$

where x_1 is determined by the equation

$$
\frac{\beta^2 x_1^2}{\tan^2\varphi} = (x - x_1)^2 - \beta^2 z^2 \quad \ldots \quad (7)
$$

and φ is the angle of sweep of the leading edge.

2.2. *Constant Load Distribution.*—The aim is to determine explicit formulae for the downwash in those cases where the load distributions vary linearly along the chord. Therefore, we consider the two distributions :

$$
l(x, y) = A = \text{const}, \quad \ldots \quad (8)
$$

$$
l(x, y) = B(x - |y| \tan\varphi). \quad \ldots \quad (9)
$$

Applying the transformations :

$$
\beta y' = \sqrt{\{(x - x')^2 - \beta^2 z^2\}} \sin\vartheta
$$

$$
t = \tan\vartheta\ ,
$$

we obtain

$$\int_0^{y_1} \frac{dy'}{(y'^2+z^2)\sqrt{\{(x-x')^2-\beta^2y'^2-\beta^2z^2\}}} = \frac{1}{(x-x')z}\tan^{-1}\frac{t_1(x-x')}{\beta z}$$

For $y_1 = x'/\tan\varphi$

$$t_1 = \frac{\beta x'}{\sqrt{[\tan^2\varphi\{(x-x')^2-\beta^2z^2\}-\beta^2x'^2]}};$$

for $y_1 = \frac{1}{\beta}\sqrt{\{(x-x')^2-\beta^2z^2\}}$

$$t_1 = \infty .$$

For constant load distribution, the potential function is thus given by the relation :

$$\frac{\phi(x,o,z)}{AV_0} = \tfrac{1}{4}(x-\beta z-x_1) + \frac{1}{2\pi}\int_0^{x_1}\tan^{-1}\frac{x'(x-x')}{z\sqrt{[\tan^2\varphi\{(x-x')^2-\beta^2z^2\}-\beta^2x'^2]}}\,dx'. \qquad (10)$$

Differentiation with respect to z gives for the downwash the relation :

$$\begin{aligned}\frac{v_z(x,o,z)}{AV_0} &= \frac{\phi_z(x,o,z)}{AV_0}\\ &= -\frac{\beta}{4} - \frac{1}{2\pi}\int_0^{x_1}\frac{\tan^2\varphi\,x'(x-x')}{(x'^2+z^2\tan^2\varphi)\sqrt{[\tan^2\varphi\{(x-x')^2-\beta^2z^2\}-\beta^2x'^2]}}\,dx'\\ &\quad + \frac{1}{2\pi}\int_0^{x_1}\frac{\beta^2x'(x-x')}{\{(x-x')^2-\beta^2z^2\}\sqrt{[\tan^2\varphi\{(x-x')^2-\beta^2z^2\}-\beta^2x'^2]}}\,dx'\\ &= -\frac{\beta}{4} + \frac{\tan^2\varphi-\beta^2}{2\pi}\int_0^{x_1}\frac{dx'}{\sqrt{[\tan^2\varphi\{(x-x')^2-\beta^2z^2\}-\beta^2x'^2]}}\\ &\quad - \frac{\tan^2\varphi}{2\pi}\int_0^{x_1}\frac{xx'+z^2\tan^2\varphi}{(x'^2+z^2\tan^2\varphi)\sqrt{[\tan^2\varphi\{(x-x')^2-\beta^2z^2\}-\beta^2x'^2]}}\,dx'\\ &\quad + \frac{\beta^2}{4\pi}(x-\beta z)\int_0^{x_1}\frac{dx'}{(x-\beta z-x')\sqrt{[\tan^2\varphi\{(x-x')^2-\beta^2z^2\}-\beta^2x'^2]}}\\ &\quad + \frac{\beta^2}{4\pi}(x+\beta z)\int_0^{x_1}\frac{dx'}{(x+\beta z-x')\sqrt{[\tan^2\varphi\{(x-x')^2-\beta^2z^2\}-\beta^2x'^2]}}\\ &= \frac{\sqrt{(\tan^2\varphi-\beta^2)}}{2\pi}\log\frac{\beta\sqrt{\{x^2+(\tan^2\varphi-\beta^2)z^2\}}}{x\tan\varphi-\sqrt{(\tan^2\varphi-\beta^2)}\sqrt{(x^2-\beta^2z^2)}}\\ &\quad - \frac{\tan^2\varphi}{2\pi}\int_0^{x_1}\frac{xx'+z^2\tan^2\varphi}{(x'^2+z^2\tan^2\varphi)\sqrt{[\tan^2\varphi\{(x-x')^2-\beta^2z^2\}-\beta^2x'^2]}}\,dx'.\end{aligned}$$

Let the following notation be introduced :

$$J_1 = \int_0^{x_1} \frac{dx'}{(x'^2 + z^2 \tan^2\varphi)\sqrt{[\tan^2\varphi\{(x-x')^2 - \beta^2 z^2\} - \beta^2 x'^2]}}, \quad \ldots \quad (11)$$

$$J_2 = \int_0^{x_1} \frac{x'\,dx'}{(x'^2 + z^2 \tan^2\varphi)\sqrt{[\tan^2\varphi\{(x-x')^2 - \beta^2 z^2\} - \beta^2 x'^2]}}. \quad \ldots \quad (12)$$

These integrals can be determined in closed form as shown in the Appendix. The final relation for the downwash then becomes :

$$\frac{v_z(x, o, z)}{AV_0} = \frac{\sqrt{(\tan^2\varphi - \beta^2)}}{2\pi} \log \frac{\beta\sqrt{\{x^2 + (\tan^2\varphi - \beta^2)z^2\}}}{x\tan\varphi - \sqrt{(\tan^2\varphi - \beta^2)}\sqrt{(x^2 - \beta^2 z^2)}}$$

$$- \frac{\tan^2\varphi}{2\pi}(xJ_2 + z^2\tan^2\varphi\, J_1). \quad \ldots \quad \ldots \quad \ldots \quad \ldots \quad \ldots \quad (13)$$

In the examples of practical interest, $z \ll x$, for most of the wing ; for this case equation (13) can be simplified considerably by using only the first-order terms with respect to z for J_1 and J_2 as given in the Appendix.

This yields :

$$\frac{v_z(x, o, z)}{AV_0} = \frac{\tan\varphi}{2\pi} \log \frac{|z|\,\beta}{2x} + \frac{\sqrt{(\tan^2\varphi - \beta^2)}}{2\pi} \log \frac{\beta}{\tan\varphi - \sqrt{(\tan^2\varphi - \beta^2)}}$$

$$+ \text{terms of order } z^2 \log|z|. \quad \ldots \quad \ldots \quad \ldots \quad \ldots \quad \ldots \quad \ldots \quad (14)$$

This equation shows that the downwash becomes logarithmically infinite for $z \to 0$.

2.3. *Linearly Varying Chordwise Load Distribution.*—For the load distribution of equation (9) we obtain for the potential function and the downwash the relations :

$$\frac{\phi(x, o, z)}{BV_0} = \tfrac{1}{8}\{(x - \beta z)^2 - x_1^2\}$$

$$+ \frac{1}{2\pi}\int_0^{x_1} x' \tan^{-1} \frac{x'(x - x')}{z\sqrt{[\tan^2\varphi\{(x-x')^2 - \beta^2 z^2\} - \beta^2 x'^2]}}\, dx'$$

$$- \frac{\tan\varphi}{2\pi}\int_0^{x_1} \frac{z}{2} \log \frac{\tan\varphi(x-x') - \sqrt{[\tan^2\varphi\{(x-x')^2 - \beta^2 z^2\} - \beta^2 x'^2]}}{\tan\varphi(x-x') + \sqrt{[\tan^2\varphi\{(x-x')^2 - \beta^2 z^2\} - \beta^2 x'^2]}} \times$$

$$\times \frac{x - x' + \sqrt{\{(x-x')^2 - \beta^2 z^2\}}}{x - x' - \sqrt{\{(x-x')^2 - \beta^2 z^2\}}}\, dx'$$

$$- \frac{\tan\varphi}{2\pi}\int_{x_1}^{x-\beta z} \frac{z}{2} \log \frac{x - x' + \sqrt{\{(x-x')^2 - \beta^2 z^2\}}}{x - x' - \sqrt{\{(x-x')^2 - \beta^2 z^2\}}}\, dx'$$

$$\frac{v_z(x,\,o,\,z)}{BV_0} = \frac{\phi_z(x,\,o,\,z)}{BV_0} = -\frac{\beta}{4}(x-\beta z)$$

$$-\frac{\tan^2\varphi}{2\pi}\int_0^{x_1}\frac{x-x'}{\sqrt{[\tan^2\varphi\{(x-x')^2-\beta^2z^2\}-\beta^2x'^2]}}\,dx'$$

$$+\frac{\beta^2}{2\pi}\int_0^{x_1}\frac{x'^2(x-x')}{\{(x-x')^2-\beta^2z^2\}\sqrt{[\tan^2\varphi\{(x-x')^2-\beta^2z^2\}-\beta^2x'^2]}}\,dx'$$

$$-\frac{\tan\varphi}{4\pi}\int_0^{x_1}\log\frac{\tan\varphi(x-x')-\sqrt{[\tan^2\varphi\{(x-x')^2-\beta^2z^2\}-\beta^2x'^2]}}{\tan\varphi(x-x')+\sqrt{[\tan^2\varphi\{(x-x')^2-\beta^2z^2\}-\beta^2x'^2]}}\,dx'$$

$$-\frac{\tan\varphi}{4\pi}\int_0^{x-\beta z}\log\frac{x-x'+\sqrt{\{(x-x')^2-\beta^2z^2\}}}{x-x'-\sqrt{\{(x-x')^2-\beta^2z^2\}}}\,dx'$$

$$+\frac{\tan\varphi}{2\pi}\int_0^{x-\beta z}\frac{x-x'}{\sqrt{\{(x-x')^2-\beta^2z^2\}}}\,dx'$$

$$=\frac{\beta^2}{4}z+\frac{\tan\varphi}{2\pi}\sqrt{(x^2-\beta^2z^2)}-\frac{\tan\varphi}{4\pi}x\log\frac{x+\sqrt{(x^2-\beta^2z^2)}}{x-\sqrt{(x^2-\beta^2z^2)}}$$

$$+\frac{\sqrt{(\tan^2\varphi-\beta^2)}}{2\pi}x\log\frac{\beta\sqrt{\{x^2+(\tan^2\varphi-\beta^2)z^2\}}}{\tan\varphi x-\sqrt{(\tan^2\varphi-\beta^2)}\sqrt{(x^2-\beta^2z^2)}}$$

$$-\frac{\beta^2}{2\pi}z\sin^{-1}\frac{z\tan\varphi}{\sqrt{\{x^2+(\tan^2\varphi-\beta^2)z^2\}}}$$

$$-\frac{\tan^4\varphi}{2\pi}z^2\int_0^{x_1}\frac{x-x'}{(x'^2+\tan^2\varphi z^2)\sqrt{[\tan^2\varphi\,\{(x-x')^2-\beta^2z^2\}-\beta^2x'^2]}}\,dx'\,.$$

Expressing the integral again by means of the integrals J_1 and J_2, as defined in equations (11) and (12), the final relation for the downwash reads :

$$\frac{v_z(x,\,o,\,z)}{BV_0} = \frac{\beta^2}{4}z+\frac{\tan\varphi}{2\pi}\sqrt{(x^2-\beta^2z^2)}$$

$$-\frac{\tan\varphi}{4\pi}x\log\frac{x+\sqrt{(x^2-\beta^2z^2)}}{x-\sqrt{(x^2-\beta^2z^2)}}$$

$$+\frac{\sqrt{(\tan^2\varphi-\beta^2)}}{2\pi}x\log\frac{\beta\sqrt{\{x^2+(\tan^2\varphi-\beta^2)z^2\}}}{\tan\varphi x-\sqrt{(\tan^2\varphi-\beta^2)}\,\sqrt{(x^2-\beta^2z^2)}}$$

$$-\frac{\beta^2}{2\pi}z\sin^{-1}\frac{z\tan\varphi}{\sqrt{\{x^2+(\tan^2\varphi-\beta^2)z^2\}}}$$

$$-\frac{\tan^4\varphi}{2\pi}z^2(xJ_1-J_2)\,. \qquad \text{(15)}$$

This relation can again be simplified for $z \ll x$:

$$\frac{v_z(x, o, z)}{BV_0} = \frac{\tan\varphi}{2\pi} x \log \frac{|z|\,\beta}{2x} + \frac{\tan\varphi}{2\pi} x$$

$$+ \frac{\sqrt{(\tan^2\varphi - \beta^2)}}{2\pi} x \log \frac{\beta}{\tan\varphi - \sqrt{(\tan^2\varphi - \beta^2)}}$$

$$- \frac{\tan^2\varphi - \beta^2}{4} z + \text{terms of order } z^2 \log |z| \,. \quad .. \quad .. \quad .. \quad (16)$$

3. *The Downwash for* $M_0 = 1$.—For a free-stream Mach number equal to unity, the analysis is very much simpler. The potential function ϕ, resulting from the linearized potential equation, is given by :

$$\phi(x, y, z) = \frac{V_0}{4\pi} z \int\int \frac{l(x', y')}{(y - y')^2 + z^2} dy'\, dx' \,, \quad .. \quad .. \quad .. \quad .. \quad .. \quad (17)$$

where the integral is to be taken over that part of the wing for which $x' < x$. Equation (17) is the limiting form of equation (4) for $\beta \to 0$. In particular, for the centre section of the wing,

$$\phi(x, o, z) = \frac{V_0}{2\pi} z \int_0^x \int_0^{x'/\tan\varphi} \frac{l(x', y')}{y'^2 + z^2} dy'\, dx' \,. \quad .. \quad .. \quad .. \quad .. \quad .. \quad (18)$$

In view of the simple relation for the potential function for sonic main-stream Mach number, we can treat chordwise load distributions which are more general than those of the previous section. We still consider the case of constant spanwise load distribution

$$l(x, y) = l(x - |y| \tan\varphi)$$

$$= l(\xi). \quad .. \quad .. \quad .. \quad .. \quad .. \quad .. \quad .. \quad .. \quad .. \quad (19)$$

It is useful to introduce ξ' and y' as independent variables into equation (18) :

$$\phi(x, o, z) = \frac{V_0}{2\pi} z \int_0^x l(\xi') \int_0^{(x-\xi')/\tan\varphi} \frac{dy'}{y'^2 + z^2} d\xi'.$$

Performing the integration over y' :

$$\phi(x, o, z) = \frac{V_0}{2\pi} \int_0^x l(\xi') \tan^{-1} \frac{x - \xi'}{z \tan\varphi} d\xi' \,.$$

Differentiation with respect to z leads to the following relation for the downwash :

$$\frac{v_z(x, o, z)}{V_0} = -\frac{1}{2\pi} \int_0^x l(\xi') \frac{(x - \xi')\tan\varphi}{(x - \xi')^2 + z^2 \tan^2\varphi} d\xi' \,. \quad .. \quad .. \quad .. \quad .. \quad (20)$$

We assume that the load distribution can be written as a polynomial in ξ :

$$l(\xi') = \sum_{n=0}^{N} a_n \xi'^n. \quad .. \quad .. \quad .. \quad .. \quad .. \quad .. \quad .. \quad .. \quad (21)$$

$l(\xi')$ can then also be written as a polynomial in $(x - \xi')$:

$$l(\xi) = \sum_{m=0}^{N} b_m(x)(x - \xi')^m \qquad (22)$$

with the coefficients :

$$b_0(x) = \sum_{n=0}^{N} a_n x^n = l(x) \qquad (23)$$

$$b_m(x) = \sum_{n=m}^{n} (-1)^m \binom{n}{m} a_n x^{n-m} . \qquad (24)$$

Inserting equation (22) into the downwash equation (20), we obtain :

$$\begin{aligned}
\frac{v_z(x, o, z)}{V_0} = &- \frac{\tan\varphi}{2\pi} b_0(x) \int_0^x \frac{x - \xi'}{(x - \xi')^2 + z^2 \tan^2\varphi} \, d\xi' \\
&- \frac{\tan\varphi}{2\pi} b_1(x) \int_0^x \frac{(x - \xi')^2}{(x - \xi')^2 + z^2 \tan^2\varphi} \, d\xi' \\
&- \frac{\tan\varphi}{2\pi} \sum_{m=2}^{N} b_m(x) \int_0^x (x - \xi')^{m-1} \, d\xi' \\
&+ \frac{\tan\varphi}{2\pi} z^2 \tan^2\varphi \sum_{m=2}^{N} b_m(x) \int_0^x \frac{(x - \xi')^{m-1}}{(x - \xi')^2 + z^2 \tan^2\varphi} \, d\xi' \\
= &\frac{\tan\varphi}{2\pi} b_0(x) \tfrac{1}{2} \log \frac{z^2 \tan^2\varphi}{x^2 + z^2 \tan^2\varphi} \\
&- \frac{\tan\varphi}{2\pi} b_1(x) \left(x - z \tan\varphi \tan^{-1} \frac{x}{z \tan\varphi} \right) \\
&- \frac{\tan\varphi}{2\pi} \sum_{m=2}^{N} b_m(x) \frac{x^m}{m} \\
&+ \text{term of order } z^2 \log |z| \\
= &\frac{\tan\varphi}{4\pi} \log \frac{z^2 \tan^2\varphi}{x^2 + z^2 \tan^2\varphi} \, l(x) \\
&- \frac{z \tan^2\varphi}{2\pi} \tan^{-1} \frac{x}{z \tan\varphi} \sum_{n=1}^{N} n a_n x^{n-1} \\
&- \frac{\tan\varphi}{2\pi} \sum_{n=1}^{N} \left[\sum_{m=1}^{n} \frac{(-1)^m}{m} \binom{n}{m} \right] a_n x^n \\
&+ \text{term of order } z^2 \log |z| . \qquad (25)
\end{aligned}$$

For the special case of linearly varying load distribution

$$l(\xi') = A + B\xi' , \qquad (26)$$

we obtain :

$$\frac{v_z(x, o, z)}{V_0} = \frac{\tan\varphi}{4\pi}(A + Bx)\log\frac{z^2\tan^2\varphi}{x^2 + z^2\tan^2\varphi} + \frac{\tan\varphi}{2\pi}Bx - \frac{\tan^2\varphi}{2\pi}zB\tan^{-1}\frac{x}{z\tan\varphi}. \quad (27)$$

For $z \ll x$:

$$\frac{v_z(x, o, z)}{V_0} = \frac{\tan\varphi}{4\pi}(A + Bx)\log\frac{z^2\tan^2\varphi}{x^2 + z^2\tan^2\varphi} + \frac{\tan\varphi}{2\pi}Bx - \frac{\tan^2\varphi}{4}zB + \text{terms of order } z^2 . \quad (28)$$

This result agrees with the limit as $\beta \to 0$ of equations (14) and (16).

4. *The Downwash in Incompressible Flow.*—In the general case of a wing with varying spanwise load distribution in incompressible flow, the wing and its wake can again be represented by a doublet distribution in the plane $z' = 0$. By this method we obtain for the velocity potential in incompressible flow the equation (*see*, for example, Ref. 1, p. 227) :

$$\phi(x, y, z) = -\frac{z}{4\pi}\int\int \frac{\phi_U(x', y') - \phi_L(x', y')}{\sqrt{\{(x - x')^2 + (y - y')^2 + z^2\}}}\,dx'\,dy',$$

where the integral has to be taken over the whole doublet distribution, *i.e.*, wing and wake. Introducing the load coefficient $l(x, y)$, equation (3), and integrating by parts with respect to x', we obtain the relation :

$$\phi(x, y, z) = -\frac{zV_0}{8\pi}\int\int \frac{l(x', y')}{(y-y')^2+z^2}\left[1 + \frac{x - x'}{\sqrt{\{(x-x')^2+(y-y')^2+z^2\}}}\right]dx'\,dy', \quad (29)$$

where the integral has to be taken over the wing area only. This equation is similar to equation (4) for supersonic flow, so that the downwash at the centre section of a swept-back wing with constant spanwise load distribution has the same singular behaviour.

However, it is easier to determine the downwash in incompressible flow by making use of the fact that a representation of the wing and its wake by a vortex distribution leads to precisely the same result as the representation by doublets (*see* Ref. 1, p. 239). We consider a wing of constant chord, with straight leading edge, infinite span and constant load distribution along lines parallel to the leading edge. This wing can be replaced by straight semi-infinite vortex lines parallel to the leading edge with the circulation

$$\Gamma = \gamma\,dn, \quad (30)$$

where

$$\gamma = \frac{l(x, y)\,V_0}{2\cos\varphi}, \quad (31)$$

$$dn = \cos\varphi\,dx'. \quad (32)$$

We make use of the Biot-Savart relation for the velocity field induced by a straight vortex line :

$$v(P) = \frac{\Gamma}{4\pi d}(\cos\vartheta_1 - \cos\vartheta_2), \quad (33)$$

where ϑ_1 and ϑ_2 are the angles between the vorticity vector and the radius vectors from the point P to the end-points of the vortex line and d is the normal distance of P from the vortex line. The velocity vector is normal to the plane through P and the vortex line.

For a point (x, o, z) and a semi-infinite vortex line from $x = y = z = 0$ swept by an angle φ :

$$d = \sqrt{(x^2 \cos^2 \varphi + z^2)} ,$$

$$\cos \vartheta_1 = \frac{x \sin \varphi}{\sqrt{(x^2 + z^2)}} ,$$

$$\cos \vartheta_2 = -1,$$

so that the velocity component parallel to the z axis :

$$dv_z = -\frac{\gamma dn}{4\pi d}(1 + \cos \vartheta_1)\frac{x \cos \varphi}{d}$$

$$= -\frac{l(x', y)\, dx'\, V_0}{8\pi} \frac{x \cos \varphi}{x^2 \cos^2 \varphi + z^2}\left\{1 + \frac{\sin \varphi x}{\sqrt{(x^2 + z^2)}}\right\}.$$

Thus we obtain for the downwash induced by the load distribution over the whole wing, equation (19),

$$\frac{v_z(x, o, z)}{V_0} = -\frac{1}{4\pi \cos \varphi}\int_0^1 l(\xi') \frac{x - \xi'}{(x - \xi')^2 + (z^2/\cos^2 \varphi)}\left[1 + \frac{\sin \varphi(x - \xi')}{\sqrt{\{(x - \xi')^2 + z^2\}}}\right] d\xi' . \quad (34)$$

The integral can be split into the following three integrals :

$$\frac{v_z(x, o, z)}{V_0} = -\frac{1}{4\pi \cos \varphi}\int_0^1 l(\xi') \frac{x - \xi'}{(x - \xi')^2 + (z^2/\cos^2 \varphi)} d\xi'$$

$$-\frac{\sin \varphi}{4\pi \cos \varphi}\int_0^1 l(\xi') \frac{d\xi'}{\sqrt{\{(x - \xi')^2 + z^2\}}}$$

$$+\frac{\sin \varphi}{4\pi \cos \varphi}\int_0^1 l(\xi') \frac{z^2/\cos^2 \varphi}{\{(x - \xi')^2 + (z^2/\cos^2 \varphi)\}\sqrt{\{(x - \xi')^2 + z^2\}}} d\xi'$$

$$= J_3 + J_4 + J_5 . \quad (35)$$

The first term, J_3, is the downwash induced by an infinite sheared wing. The second term, J_4, has for small z a singularity like $l(x) \log z$. The third term, J_5, has a value proportional to $l(x)$ for small z.

For a linearly varying load distribution

$$l(\xi') = A + B\xi', \quad (26)$$

the integrals have the values :

$$J_3 = -\frac{1}{4\pi \cos \varphi}\left\{\frac{A + Bx}{2} \log \frac{x^2 + (z^2/\cos^2 \varphi)}{(1 - x)^2 + (z^2/\cos^2 \varphi)}\right.$$

$$\left. - B - B\frac{z}{\cos \varphi} \tan^{-1} \frac{z/\cos \varphi}{x(1 - x) - (z^2/\cos^2 \varphi)}\right\}, \quad (36)$$

$$J_4 = -\frac{\sin\varphi}{4\pi\cos\varphi}\left[(A+Bx)\log\frac{\sqrt{(x^2+z^2)}+x}{\sqrt{\{(1-x)^2+z^2\}}-(1-x)}\right.$$

$$\left.+B\sqrt{\{(1-x)^2+z^2\}}-B\sqrt{(x^2+z^2)}\right], \quad .. \quad .. \quad .. \quad .. \qquad (37)$$

$$J_5 = \frac{1}{4\pi\cos\varphi}\times$$

$$\times\left\{\frac{A+Bx}{2}\log\frac{\{\sqrt{(x^2+z^2)}+x\sin\varphi\}[\sqrt{\{(1-x)^2+z^2\}}+(1-x)\sin\varphi]}{\{\sqrt{(x^2+z^2)}-x\sin\varphi\}[\sqrt{\{(1-x)^2+z^2\}}-(1-x)\sin\varphi]}\right.$$

$$-B\frac{z}{\cos\varphi}\tan^{-1}\frac{z\tan\varphi}{\sqrt{\{(1-x)^2+z^2\}}}$$

$$\left.+B\frac{z}{\cos\varphi}\tan^{-1}\frac{z\tan\varphi}{\sqrt{(x^2+z^2)}}\right\}. \quad .. \quad .. \quad .. \quad .. \quad .. \qquad (38)$$

The values for z small compared with x, $1-x$, and 1 are

$$\lim_{z\to 0} J_3 = -\frac{1}{4\pi\cos\varphi}\left\{(A+Bx)\log\frac{x}{1-x}-B\right\}, \quad .. \quad .. \quad .. \quad .. \qquad (39)$$

$$\lim_{z\to 0} J_4 = -\frac{\sin\varphi}{4\pi\cos\varphi}\left\{(A+Bx)\log\frac{4x(1-x)}{z^2}+B-2Bx\right\}, \quad .. \qquad (40)$$

$$\lim_{z\to 0} J_5 = \frac{1}{4\pi\cos\varphi}(A+Bx)\log\frac{1+\sin\varphi}{1-\sin\varphi}. \quad .. \quad .. \quad .. \quad .. \quad .. \qquad (41)$$

5. *Approximate Method of Satisfying the Boundary Condition at the Surface of the Wing.*— The boundary condition that the aerofoil surface is a stream surface, *i.e.*, that the total velocity component normal to the surface is zero, can be written in the form

$$dx : dy : dz = V_x : V_y : V_z .$$

The projection of the stream surface on a plane $y = \text{const}$ is thus given by the relation :

$$\frac{dz(x,y)}{dx} = \frac{V_{z0}+v_z(x,y,z)}{V_{x0}+v_x(x,y,z)}, \quad .. \quad .. \quad .. \quad .. \quad .. \quad .. \quad .. \qquad (42)$$

where $z = z(x, y)$ determines the aerofoil surface, V_{x0} and V_{z0} are the components of the free stream velocity V_0 with respect to the x and z axis and v_x and v_z are the perturbation velocities.

In ordinary linear aerofoil theory, this condition is approximated by the following condition in the chordal plane, $z = 0$:

$$\frac{dz(x,y)}{dx} = \frac{V_{z0}+v_z(x,y,o)}{V_0}. \quad .. \quad .. \quad .. \quad .. \quad .. \quad .. \quad .. \qquad (43)$$

This means that the assumptions are made that the velocity component v_z does not vary much between the chordal plane and the wing surface, that the velocity increment $v_x(x, y, z)$ is small compared to the x component of the free-stream velocity, V_{x0}, and that the angle between the main-stream direction and the plane $z = 0$ is small so that V_{x0} can be approximated by V_0.

In our case, we are still entitled to make the second and third assumptions, provided the load is finite or zero at the leading and trailing edges. But equations (35), (37) and (40) show that the downwash at the centre section, $y = 0$, becomes logarithmically infinite when $z \to 0$. This is also true at sonic speed, as can be seen from equations (25), (27), (28), and in supersonic flow, as follows from equations (13) to (16) and the singular behaviour of the integrals J_1 and J_2 for $z \to 0$. This implies that an infinitely thin wing, which gives the required load distribution (constant along lines $\xi = x - |y| \tan \varphi = \text{const}$) would have a singular behaviour of its surface slopes at $y = 0$. Such a wing cannot be represented by a plane sheet of vortices or doublets.

At this point, we must remind ourselves that our aim is to design wings of finite thickness. Thin cambered wings and thickness distributions are designed separately and subsequently superimposed only when this implies a simplification, which it does not in the present case. To represent cambered and twisted wings of finite thickness requires a source-sink distribution and a doublet or vortex distribution within the wing or at its surface, such that after superimposing the parallel main flow the wing surface is a stream surface. The flow outside the wing must be free of singularities but a singular behaviour of the flow inside the wing is of no importance. We do not attempt to solve the problem fully since this would involve source and doublet distributions on curved surfaces, but we expect to obtain a reasonable approximation by retaining plane sheets of singularities.

To solve this problem, let us first consider an iteration process by which we can obtain an exact solution for the two-dimensional case by means of singularities. The procedure is similar to that described in Section 3-5 of Ref. 2 for determining the flow past a thin air intake with axial symmetry. To determine the flow around a thin wing with given load distribution, we can start with a plane vortex sheet in the plane $z = 0$, superpose a flow parallel to the plane $z = 0$, and determine the stream surfaces as shown in Fig. 2. Some stream surfaces cross the vortex sheet and have a discontinuity of slope there (*see* also Fig. 3-3 of Ref. 2). For the next step in the iteration process we choose an approximate shape for the aerofoil, *e.g.*, the stream surface $z^*(x)$ through the leading edge obtained in the first step. With the singularities on this surface, we calculate a second approximation for the aerofoil shape and so on until the sheet with the vortices and the stream surface coincide.

Let us now compare this final result with the approximate one obtained from the plane vortex sheet through the leading and trailing edges of the wing. The velocity components normal to the sheet induced by the curved sheet do not differ much from those induced by the plane sheet at the same distance from the sheet, as long as the curvature of the curved sheet is not too large. An approximation to the aerofoil is thus obtained by calculating the velocity component normal to the plane sheet at the sheet and by superposing a parallel flow at the incidence α_T to the sheet (*see* Fig. 2). The velocity components normal to the plane sheet are, of course, the same as the velocity components $v_z(x, o)$ which a sheet in the plane $z = 0$ induces in the plane $z = 0$. The angle α_T is found from the relation

$$\alpha_T = \tan^{-1} \{ - z(x = 1) \} . \quad . . \quad . . \quad . . \quad . . \quad . . \quad . . \quad . . \quad (44)$$

The aerofoil surface can be determined from

$$z(x) = \int_0^x \frac{v_z(x', o)}{V_0} \, dx', \quad . . \quad . . \quad . . \quad . . \quad . . \quad . . \quad . . \quad . . \quad (45)$$

if the incidence α_T is small so that the velocity component $V_0 \cos \alpha_T$ parallel to the sheet can be approximated by V_0.

That the error due to the neglect of the curvature of the sheet is small, for practical values of the maximum camber, f, has been shown, *e.g.*, in Ref. 3 by comparing the exact velocity component $V(x)/V_0$ along circular-arc aerofoils ($f = 0{\cdot}02$ and $0{\cdot}04$) in a flow parallel to the chord, with the approximate one.

Equation (45) is usually a better approximation than the stream surface $z^*(x)$ through the leading edge obtained in the first step for the plane sheet in $z = 0$ (*see* also Fig. 3-4 in Ref. 2). The velocity components induced by the plane sheet in $z = 0$ on the stream surface $z^*(x)$ usually differ more from those induced on $z = 0$ than the difference due to ignoring the curvature of the sheet, unless α_T is rather small.

With thick cambered wings in two-dimensional flow, the iteration process could be similar to that for thin wings. We can start with a source distribution and a vortex distribution in the plane $z = 0$, superpose the flow parallel to the x axis and determine the stream surface passing through the stagnation line. In the next step the singularities are placed on the mean surface, $z^*(x)$, of the stream surface obtained in the first step and so on until a stream surface is obtained which contains all singularities inside it. Whether the sources and vortices are to be placed on the same surface or not is here irrelevant. As an approximation to the singularities on the final mean surface we can again take plane sheets through the leading and trailing edges, as long as the curvature of the mean surface is not too large. Neglecting the curvature of the sheets will involve only small errors in the velocity components. In the two-dimensional case the velocity components due to source and vortex sheets do not vary much with the distance from the sheets in the neighbourhood of the sheets except near the edges of the sheets. This can be seen, *e.g.*, from equation (36), since J_3 gives for incompressible two-dimensional flow the v_z velocity induced by a vortex sheet in $z = 0$ of linearly varying strength. This implies that we can calculate the velocity components either on the sheet itself (as is done in ordinary linear theory) or at a distance equal to half the local wing thickness. This approximate procedure ensures that, for the ordinary range of wing thickness and maximum camber, there are no singularities outside the stream surface.

Let us now return to our three-dimensional problem. The iteration procedure would lead to a mean surface which is curved in planes $y = \text{const}$ as well as in planes $x = \text{const}$. Assuming again in this case that neglecting the curvature of the sheet of singularities does not involve large errors in the velocity components, we represent for the calculation of the centre section the curved sheet by a plane sheet through the line $x = z = 0$ and the trailing edge of the centre section. The only important difference from the two-dimensional case is that for the centre section, $y = 0$, we calculate the velocity component v_z induced by the vortices at the surface of the thick wing and not at the plane $z = 0$. This refinement, which would be of negligible importance for the two-dimensional wing, is essential when a singular behaviour of v_z occurs at the plane $z = 0$, i.e., when the velocity v_z varies considerably with the distance z. It is a legitimate means of evading the singularity since we have to satisfy the boundary condition at the surface of the thick wing anyway.

This method is similar to the method of calculating the velocity distribution at the surface of slender bodies of revolution by means of sources on the axis. The term rv_r (where v_r is the radial velocity component), which occurs in the boundary condition, is regular at the axis and is therefore taken at the axis instead of at the surface, but the axial component, v_x, being singular the axis, is taken at the surface. In our case, the v_x component due to the doublets, being regular at $z = 0$, is taken at $z = 0$; v_z, being singular at $z = 0$, is taken at the surface.

The velocity v_z is calculated at a distance z_t from the plane $z = 0$, where :

$$z = z_t(x, y) = \tfrac{1}{2}[z_U(x, y) - z_L(x, y)] \qquad (46)$$

determines the thickness distribution, and not at the distance z_U and z_L of the upper and lower surfaces of the aerofoil. In a proper representation of the cambered thick aerofoil the distance between the surface and the position of the singularities is, at least approximately, z_t.

To summarize : we calculate first the velocity $v_z(x, o, z_t)$ which a sheet of doublets in $z = 0$ induces at $z = z_t$; then determine

$$z(x, o) = \int_0^x \frac{v_z(x', o, z_t)}{V_0}\, dx' \qquad (47)$$

and write $z(x, o)$ in the form

$$z(x, o) = -\tan \alpha_T x + z_c(x, o) \quad \ldots \quad (48)$$

with

$$\tan \alpha_T = -z(x = 1, 0). \quad \ldots \quad (49)$$

$z_c(x, o)$ gives the camber line and α_T the twist for the centre section of the wing. This procedure gives a solution correct to the first order. Second-order terms are ignored, *e.g.*, the interference between thickness and camber terms (*i.e.*, source and vortex distributions), and the effect of the varying twist and camber along the span (*i.e.*, the curvature of the vortex sheets).

6. *Calculated Examples.*—6.1. *Effect of the Free-Stream Mach Number M_0.*—Some typical calculations have been made for a wing with 55-deg sweep of the leading edge and an RAE 101 thickness distribution of thickness/chord ratio 0·045. The load distributions chosen were :

$$l(\xi) = 0{\cdot}4 - 0{\cdot}3\xi, \qquad \xi = x - |y| \tan \varphi \quad \ldots \quad (50)$$

$$l(\xi) = 0{\cdot}5(1 - \xi). \quad \ldots \quad (51)$$

The total load is the same for the two examples, $C_L(y) = 0{\cdot}25$.

The downwash $v_z(x, o, z_t)$ induced at the surface of the wing is plotted in Figs. 3 and 4 for three different Mach numbers. For $M_0 = 0$ and finite load at the leading or trailing edges, the downwash is logarithmically infinite at these edges. Such a logarithmic singularity occurs also on the two-dimensional wing with finite load at the edges. For $M_0 = 1$, the downwash at the leading edge is zero for sections with rounded noses ; it is finite for sections with sharp but non-cusped edges. At the trailing edge v_z is logarithmically infinite for finite load at the trailing edge and it is finite for zero load. For supersonic flow the downwash is zero at the point for which $x^* = \beta z_t(x^*)$ and the points upstream, $0 < x < x^*$; at the trailing edge the downwash is again logarithmically infinite for finite load and finite for zero load. Since the determination of the downwash near the leading edge is not very accurate by the present method, we have calculated the values of v_z for $x > 0{\cdot}02$ at $M_0 = 0$ and $M_0 = 1{\cdot}2$, and have extrapolated the $z(x)$ values obtained by integrating the v_z calculated over the range $0{\cdot}02 < x < 1{\cdot}0$ by a smooth curve. The resulting mean surfaces and the camber lines are plotted in Figs. 3 to 5. The angles of twist, α_T, are quoted in Figs. 3 and 4.

Figs. 3 to 5 show that the downwash distributions and the resulting section shapes are surprisingly similar for incompressible flow and supersonic main stream. That the result for sonic speed lies roughly between the two others was to be expected since we get the same limit for the potential equation, equation (17), when we approach $M_0 = 1$ from the supersonic range as when we approach it from the subsonic one†.

Since the calculations for $M_0 = 1$ are much simpler than for $M_0 \neq 1$, this similarity between the results at $M_0 = 1$ and low supersonic speeds can be made use of, if one requires a qualitative answer about the effect of varying certain parameters, *e.g.*, the type of loading, the plan-form, or the thickness distribution of the wing.

---

† For subsonic flow, by means of the Prandtl-Glauert analogy

$$\phi(x, y, z) = \frac{1}{\beta^2}\phi_c(x, \beta y, \beta z)$$

the potential equation reads instead of equation (29) :

$$\phi(x, y, z) = -\frac{zV_0}{8\pi}\iint \frac{l(x', y')}{(y - y')^2 + z^2}\left[1 + \frac{x - x'}{\sqrt{\{(x - x')^2 + \beta^2(y - y')^2 + \beta^2 z^2\}}}\right]dx'\,dy'$$

with $\beta = \sqrt{(1 - M_0^2)}$.

The section shapes $z(x)$ obtained for the chosen load distributions (*see* Figs. 3 and 4) are composed mainly of a twist term and of only a small camber term. This implies that neglecting the chordwise curvature of the vortex sheet in our approximate method should be justifiable. The amount of the spanwise curvature of the mean surface can be obtained from the results quoted in Section 7.

6.2. *Effect of the Load Distribution.*—The effect of altering the chordwise load distribution is illustrated in Fig. 6. The distribution has been varied between a constant one and one decreasing linearly to zero at the trailing edge. The total load is the same for the three cases. The twist varies by only 6 per cent of its total value, but the shape of the camber-line and the maximum camber depend very much on the load distribution. The same holds for all Mach numbers as shown by Fig. 5 and a comparison of Figs. 3 and 4.

Sometimes a modification of the resulting camber-line may be required. Such a modification imposes the question of how much the load distribution would be altered. An estimate of this variation may be obtained by determining from the modified camber-line the required change of the downwash at a few chordwise positions and solving the resulting system of linear equations between the downwash at $M_0 = 1$ and the coefficients a_n in equations (21) and (25).

6.3. *Effect of the Wing Thickness.*—Retaining the thickness distribution but altering the thickness/chord ratio, we obtain for a fixed load distribution from the approximate relations (14) and (16) for supersonic flow the relation

$$\frac{v_x(x\,;\,t/c)}{V_0} = \frac{v_z(x\,;\,t_0/c)}{V_0} + (A + Bx)\frac{\tan\varphi}{2\pi}\log\frac{t/c}{t_0/c} - B\frac{t/c - t_0/c}{t_0/c}\,\frac{\tan^2\varphi - \beta^2}{4}\,z(t_0/c)\,.$$

For aerofoils of practical interest this relation can be approximated by :

$$\frac{v_x(x\,;\,t/c)}{V_0} = \frac{v_z(x\,;\,t_0/c)}{V_0} + (A + Bx)\frac{\tan\varphi}{2\pi}\log\frac{t/c}{t_0/c}\,. \qquad (52)$$

The same relation is obtained for $M_0 = 1$ by equation (28) and for $M_0 = 0$ by equations (35), and (39) to (41). The variation of the downwash with the thickness/chord ratio is thus to a first order independent of the Mach number and proportional to the load distribution. In particular,

$$\tan\alpha_T(t/c) = \tan\alpha_T(t_0/c) - \frac{\tan\varphi}{2\pi}\left(A + \frac{B}{2}\right)\log\frac{t/c}{t_0/c}\,, \qquad (53)$$

and

$$z_c(x\,;\,t/c) = z_c(x\,;\,t_0/c) - \frac{\tan\varphi}{2\pi}\,\frac{B}{2}\log\frac{t/c}{t_0/c}\;x(1-x)\,. \qquad (54)$$

For $M_0 = 1$ the downwash has also been calculated for various thickness/chord ratios by the exact equation (27). The resulting angle of twist is compared in Fig. 7 with approximation (53) and the camber-lines in Fig. 8 with approximation (54). $t_0/c = 0{\cdot}03$ was taken for the basic solution.

6.4. *Effect of the Angle of Sweep.—Comparison with an Approximate Formula for the Downwash in Incompressible Flow.*—Downwash distributions (divided by $\tan\varphi$) for various angles of sweep are plotted in Figs. 9a and 9b for the case of incompressible flow. The corresponding section shapes, the angles of twist and the camber lines are given in Figs. 10, 11 and 12. The level of the downwash and with it the angle of twist increase with increasing angle of sweep. The same is true for sonic and supersonic flow. A simple approximation for the variation of the downwash with the angle of sweep can be derived for sonic speed by equation (28). For small values of z :

$$\frac{v_z(x\,;\varphi)}{V_0} = \tan\varphi\,\frac{v_z(x\,;\varphi = 45°)}{V_0} + \tan\varphi\,\log\tan\varphi\,\frac{A + Bx}{2\pi} \quad . \quad . \quad . \quad . \quad . \quad . \quad . \quad (55)$$

To obtain a simple method for calculating the chordwise and spanwise load distributions on swept wings with given geometry in incompressible flow, an approximation to the downwash induced by a given load distribution was used in Refs. 4 and 7. As a start, the downwash at the centre section of a swept wing of infinite aspect ratio with constant spanwise load distribution (*i.e.*, the case considered in this note) was approximated by (*see*, for example, Refs. 4 to 7) :

$$\frac{v_z(x,\,o)}{V_0} = -\frac{1}{2\pi}\int_0^1 \frac{\gamma(\xi')}{V_0}\,\frac{d\xi'}{x - \xi'} - \sigma\,\frac{\gamma(x)}{2\pi V_0} \quad . \quad . \quad . \quad . \quad . \quad . \quad (56)$$

with

$$\sigma = \pi\tan\varphi\,, \quad . \quad . \quad . \quad . \quad . \quad . \quad . \quad . \quad . \quad (57)$$

where the vortex strength $\gamma(x)$ and the load distribution are related by equation (31). Equation (56) approximates the downwash at the position x of the centre section by the sum of the downwash on the two-dimensional wing and a term proportional to the local vortex strength, $\gamma(x)$. Such a form, as a crude approximation, is also suggested by equations (35) and (39) to (41). J_3 is the downwash of the corresponding sheared wing and the term in J_4 which becomes most important for $z \to 0$ is proportional to the local load and J_5 is proportional to the local load.

The approximation (56) has been derived in Refs. 4 to 7 for wings of moderate sweep ($\varphi \leqq 45$ deg), wings of a thickness/chord ratio of about $0{\cdot}1$ and for the vortex distributions of the flat plate

$$\gamma(\xi) = \text{const}\,\sqrt{\left(\frac{1-\xi}{\xi}\right)},$$

and for the elliptic vortex distribution

$$\gamma(\xi) = \text{const}\,\sqrt{\{1 - (1 - 2\xi)^2\}}.$$

It is, therefore, of interest to see how good an approximation equations (56) and (57) are for other cases, *e.g.*, for wings with higher angles of sweep, for thinner wings, for different load distributions. With the special load distribution

$$l(\xi) = 2\cos\varphi\,\frac{\gamma(\xi)}{V_0} = A + B\xi,$$

equation (56) reads :

$$\frac{v_z(x,\,o)}{V_0} = -\frac{1}{4\pi\cos\varphi}\left\{(A + Bx)\log\frac{x}{1-x} - B + \pi\tan\varphi(A + Bx)\right\}. \quad . \quad . \quad (58)$$

The downwash distributions calculated by equations (35), (39) to (41), and by approximation (58), are plotted together in Figs. 9a and 9b. The section shapes, the angles of twist and the camber-lines determined from the various downwash distributions are plotted in Figs. 10, 11 and 12. For moderate angles of sweep the differences in the angles of twist are tolerable for a crude approximation. The shapes of the camber-lines differ more than the angles of twist, as is to be expected. The approximation (58) becomes less valid with increasing angle of sweep. Expressing v_z as given by equations (35), and (39) to (41), in the form of equation (56), we obtain for σ the value

$$\sigma = \sin\varphi \left\{ \log \frac{4x(1-x)}{z^2} + \frac{B - 2Bx}{A + Bx} \right\} - \log \frac{1 + \sin\varphi}{1 - \sin\varphi} . \qquad (59)$$

The large discrepancy between the approximate formula (58) and the exact results for large angles of sweep is due to the fact that $\sigma = \pi \tan\varphi$, equation (57), tends to infinity as $2/(1 - \varphi/\frac{1}{2}\pi)$ for $\varphi \to \frac{1}{2}\pi$, whilst σ by equation (59) tends to infinity as $2 \log \{\frac{1}{4}\pi(1 - \varphi/\frac{1}{2}\pi)\}$.

The original approximation for σ (*see* Ref. 4) was

$$\sigma = 2\pi \sin\varphi \, \sigma^* - \log \frac{1 + \sin\varphi}{1 - \sin\varphi} , \qquad (60)$$

where σ^* was taken to be independent of x. σ^* is a function of the thickness/chord ratio. A comparison of equations (59) and (60) leads to the relation

$$\sigma^*(t/c) = \sigma^*(t_0/c) - \frac{1}{\pi} \log \frac{t/c}{t_0/c} . \qquad (61)$$

Taking $\sigma^*(t_0/c = 0{\cdot}1) = 1{\cdot}0$, we obtain the approximation :

$$\sigma^*(t/c) = 1 - \frac{1}{\pi} \log (10\, t/c) . \qquad (62)$$

The approximation for v_z obtained by equations (56) (60) and (62) is also plotted in Figs. 9a and 9b, and the resulting section shapes, angles of twist and camber-lines in Figs. 10, 11 and 12. The angles of twist agree surprisingly well with the exact values but there are large differences in the shape of the camber-lines between the approximate and the exact solutions. However, the angle of twist is the more important term, as illustrated in Fig. 10. The results in Figs. 10 to 12 are, of course, affected by the particular chordwise loading and section shape chosen and are, therefore, not necessarily general. Other cases are considered in Ref. 7.

It may be mentioned here that experiments at low speed have proved that a wing with approximately constant spanwise load distribution can be obtained by the present simple method. A cambered and twisted 45-deg swept-back wing has been designed by applying equations (56) and (57) so as to have the flat-plate load distribution over the whole wing. The measured pressure distributions at the centre section and at a spanwise station away from centre and tip agree within the accuracy of the experiment (*see* Ref. 6).

7. *The Shape of the Aerofoil at Stations away from the Centre Section.*—The downwash induced by a plane sheet of doublets and hence the required slope of the wing varies, of course, with the distance from the centre section. To show this variation, we consider the case of sonic main flow since it is so much simpler to calculate than the cases of subsonic or supersonic main flow. We may expect that the results will hold qualitatively also for $M_0 \neq 1$, as was true for the centre section.

We apply equation (17) to the load distribution

$$l(x, y) = A + B(x - |y| \tan \varphi) \qquad (63)$$

and a constant-chord swept-back wing. Integrating with respect to y', differentiating with respect to z and integrating with respect to x', we obtain for points in front of the trailing edge of the centre section, $x < 1$:

$$\frac{v_z(x, y, z)}{V_0} = -\frac{\tan \varphi}{8\pi}\left[\{A + B(x + y \tan \varphi)\} \log \frac{(x + y \tan \varphi)^2 + z^2 \tan^2 \varphi}{\tan^2 \varphi (y^2 + z^2)}\right.$$

$$+ \{A + B(x - y \tan \varphi)\} \log \frac{(x - y \tan \varphi)^2 + z^2 \tan^2 \varphi}{\tan^2 \varphi (y^2 + z^2)}$$

$$\left. + 2Bz \tan \varphi \left(\tan^{-1} \frac{x + y \tan \varphi}{z \tan \varphi} + \tan^{-1} \frac{x - y \tan \varphi}{z \tan \varphi}\right) - 4Bx\right] \qquad (64)$$

and for $x > 1$:

$$\frac{v_z(x, y, z)}{V_0} = -\frac{\tan \varphi}{8\pi}\left[\{A + B(x + y \tan \varphi)\} \log \frac{(x + y \tan \varphi)^2 + z^2 \tan^2 \varphi}{(x - 1 + y \tan \varphi)^2 + z^2 \tan^2 \varphi}\right.$$

$$+ \{A + B(x - y \tan \varphi)\} \log \frac{(x - y \tan \varphi)^2 + z^2 \tan^2 \varphi}{(x - 1 - y \tan \varphi)^2 + z^2 \tan^2 \varphi}$$

$$+ 2Bz \tan \varphi \left(\tan^{-1} \frac{x + y \tan \varphi}{z \tan \varphi} + \tan^{-1} \frac{x - y \tan \varphi}{z \tan \varphi}\right.$$

$$\left.\left. - \tan^{-1} \frac{x - 1 + y \tan \varphi}{z \tan \varphi} - \tan^{-1} \frac{x - 1 - y \tan \varphi}{z \tan \varphi}\right) - 4B\right]. \qquad (65)$$

The limit of $v_z(x, y, z)$ as z tends to zero is finite for $y \neq 0$.

$x < 1$:

$$\frac{v_z(x, y, o)}{V_0} = -\frac{\tan \varphi}{4\pi}\left[\{A + B(x + y \tan \varphi)\} \log \frac{x + y \tan \varphi}{y \tan \varphi}\right.$$

$$\left. + \{A + B(x - y \tan \varphi)\} \log \frac{x - y \tan \varphi}{y \tan \varphi} - 2Bx\right], \qquad (66)$$

$x > 1$:

$$\frac{v_z(x, y, o)}{V_0} = -\frac{\tan \varphi}{4\pi}\left[\{A + B(x + y \tan \varphi)\} \log \frac{x + y \tan \varphi}{x - 1 + y \tan \varphi}\right.$$

$$\left. + \{A + B(x - y \tan \varphi)\} \log \frac{x - y \tan \varphi}{x - 1 - y \tan \varphi} - 2B\right]. \qquad (67)$$

For stations far away from the centre section, $y \to \infty$, we obtain from equation (67)

$$\frac{v_z(\xi, z = 0)}{V_0} = -\frac{\tan \varphi}{4\pi}\left\{(A + B\xi) \log \frac{\xi}{1 - \xi} - B\right\}, \qquad (68)$$

where

$$\xi = x - y \tan \varphi .$$

The same result is obtained for an infinite sheared wing, with a load distribution $l(\xi) = A + B\xi$, by considering the subsonic flow around the two-dimensional wing normal to the leading edge.

For the load distribution $l(\xi) = 0{\cdot}4 - 0{\cdot}3\xi$, the downwash has been calculated at the stations $y = 0{\cdot}025, 0{\cdot}05, 0{\cdot}1, 0{\cdot}2$, by equations (64) to (67). The results, plotted in Fig. 13, show that the difference between the downwash at the surface of the wing, $z = z_t$, and the downwash in the chordal plane, $z = 0$, is negligible for $y \geq 0{\cdot}1$. The resulting camber-lines and angles of twist are plotted in Figs. 14 and 15. The angle of twist changes rather rapidly along the span. It was suggested in Ref. 7 that the distortion of the load distribution at and near the centre section from that further out on the wing, and in particular the shift of the aerodynamic centre, of a flat swept-back wing at incidence follow a law containing only the spanwise co-ordinate y in terms of the local chord and the angle of sweep, as follows :

$$\lambda(y) = \sqrt{\left\{1 + \left(2\pi \frac{\tan\varphi}{\varphi} y\right)^2\right\}} - 2\pi \frac{\tan\varphi}{\varphi} y \,. \qquad \ldots \qquad \ldots \qquad \ldots \qquad \ldots \qquad (69)$$

Fig. 15 shows that the angle of twist obtained by a calculation for $M_0 = 1$ varies in a similar fashion. The rapid change of the angle of twist implies that the spanwise curvature of the aerofoil mean surface is not small near the centre of the wing. This means that our approximation of replacing the actual curved mean surface by a plane one with the local angle of twist leads to results near the centre which may be less accurate than for the two-dimensional wing or for stations further outboard.

It is known from experiments (*see*, for example, Fig. 25 in Ref. 8) that in incompressible flow the pressure distribution over a flat swept-back wing at incidence is such that at and near the centre of the wing a normal pressure drag is produced which decreases along the span. This pressure drag is partly cancelled by thrust forces at the wing tips such that for a wing of finite aspect ratio the total remaining drag is equal to the vortex drag, plus a contribution caused by the viscosity of the flow.

A normal pressure drag occurs also near the centre of cambered and twisted wings with constant spanwise load distributions in incompressible, sonic and supersonic flow. The sectional drag coefficient for a thin wing of constant chord is related to the pressure distribution and to the wing shape by the equation

$$C_D(y) = C_L(y)\, \alpha_T(y) - \int_{x_{L.E.}}^{x_{T.E.}} l(x, y)\, \frac{dz_c(x, y)}{dx}\, dx .$$

The numerical results of Figs. 3, 4, 14 and 15 show that, for the load distributions considered, the angle of twist is much larger than the maximum camber for stations near the centre. This means that the term $C_L\alpha_T$ gives the main contribution to the drag and that the spanwise variation of the pressure drag is similar to the $\lambda(y)$ curve.

It was found from Figs. 3 and 4 that the section shape at the centre section does not vary much with the free-stream Mach number. As a consequence the sectional pressure drag at the centre section is nearly the same for incompressible and low supersonic speeds. However, we cannot draw any conclusions regarding the value of the total drag of a finite aspect ratio wing since the forces at the wing tips vary considerably with the free-stream Mach number.

8. *Wing-body Combinations with Constant Spanwise Load Distribution Over the Wing.*—The singular behaviour of the downwash on the chord-line of the centre section is not a property of the isolated wing but occurs also at the junction of a fuselage and a swept wing which has (in the presence of the fuselage) the same chordwise load distribution at all spanwise stations right up to the junction.

This can be illustrated by considering a cylindrical fuselage at zero incidence in mid-wing position. The wing is cambered and twisted so that the load distribution $l(x, y)$ is constant, $= A$, over the whole wing. The discontinuity in the velocity potential

$$\Delta\phi(x, y) = \phi_U(x, y) - \phi_L(x, y)$$

is then determined by equation (3). Thus

$$\frac{\Delta\phi(x, y)}{V_0} = A\tfrac{1}{2}(x - x_{LE})$$

$$= A\tfrac{1}{2}(x - |y| \tan\varphi) \,. \qquad \ldots \quad \ldots \quad \ldots \quad \ldots \quad \ldots \quad \ldots \qquad (70)$$

To determine the downwash field we apply slender-body theory, *i.e.*, we determine, for each cross-sectional plane $x = \text{const}$, the two-dimensional flow which satisfies the boundary condition (70) for the velocity potential. We assume that the loading is small, *i.e.*, that camber and twist are small so that a cross-section through the wing can be approximated by a straight line. We consider only the cross-sections in front of the trailing edge of the wing-body junction.

The two-dimensional problem is best solved by transforming the plane $x = \text{const}$,

$$\zeta = y + iz$$

into a $\bar{\zeta}$ plane by the transformation

$$\bar{\zeta} = \zeta - \frac{R^2}{\zeta} \,, \qquad \ldots \quad \ldots \quad \ldots \quad \ldots \quad \ldots \quad \ldots \quad \ldots \quad \ldots \qquad (71)$$

so that the body contour, $|\zeta| = R$, is transformed into the slit $\bar{y} = 0$, $|\bar{z}| < 2R$. The wing is transformed into the straight line $|\bar{y}| < s(x) - R^2/s(x)$, $\bar{z} = 0$, where $s(x) = x/\tan\varphi$. Points on the original and the transformed wing contour are related by

$$y = \tfrac{1}{2}\{\bar{y} + \sqrt{(\bar{y}^2 + 4R^2)}\} \,. \qquad \ldots \quad \ldots \quad \ldots \quad \ldots \quad \ldots \quad \ldots \qquad (72)$$

The transformation does not alter the value of the discontinuity in the velocity potential so that by equations (70) and (72) :

$$\frac{\Delta\phi(\bar{y}, \bar{z} = 0\,; x)}{V_0} = \frac{A}{4}\{2x - |\bar{y}| \tan\varphi - \tan\varphi \sqrt{(\bar{y}^2 + 4R^2)}\} \,. \ldots \quad \ldots \quad \ldots \quad \ldots \qquad (73)$$

The flow which satisfies equation (73) induces at $\bar{z} = 0$ the downwash :

$$\frac{\bar{v}_{\bar{z}}(x, \bar{y}, o)}{V_0} = -\frac{1}{2\pi}\int_{-\bar{s}}^{\bar{s}} \frac{\partial\Delta\phi(\bar{y}')/V_0}{\partial\bar{y}'}\frac{d\bar{y}'}{\bar{y} - \bar{y}'}$$

$$= +\frac{A}{8\pi}\tan\varphi\int_{-\bar{s}}^{0}\left\{\frac{\bar{y}'}{\sqrt{(\bar{y}'^2 + 4R^2)}} - 1\right\}\frac{d\bar{y}'}{\bar{y} - \bar{y}'}$$

$$+\frac{A}{8\pi}\tan\varphi\int_{0}^{\bar{s}}\left\{\frac{\bar{y}'}{\sqrt{(\bar{y}'^2 + 4R^2)}} + 1\right\}\frac{d\bar{y}'}{\bar{y} - \bar{y}'},$$

which gives

$$\frac{\bar{v}_{\bar{z}}}{V_0} = \frac{A}{8\pi}\tan\varphi\left[\left\{1+\frac{\bar{y}}{\sqrt{(\bar{y}^2+4R^2)}}\right\}\log\frac{\bar{y}^2}{s^2-\bar{y}^2}\right.$$

$$+2\left\{1-\frac{\bar{y}}{\sqrt{(\bar{y}^2+4R^2)}}\right\}\log 2R$$

$$-2\log\{\sqrt{(\bar{s}^2+4R^2)}+\bar{s}\}$$

$$\left.+\frac{\bar{y}}{\sqrt{(\bar{y}^2+4R^2)}}\log\frac{2\bar{y}^2\bar{s}^2+4R^2(\bar{y}^2+s^2)+2\bar{y}\bar{s}\sqrt{(\bar{y}^2+4R^2)}\sqrt{(\bar{s}^2+4R^2)}}{\bar{y}^2}\right]. \quad (74)$$

The v_z velocity in the original plane is related to $\bar{v}_{\bar{z}}$ in the transformed plane by the mapping ratio $|d\bar{\zeta}/d\zeta|$:

$$v_z(x, y, z=0) = \bar{v}_{\bar{z}}\left|\frac{d\bar{\zeta}}{d\zeta}\right|$$

$$=\left(1+\frac{R^2}{y^2}\right)\bar{v}_{\bar{z}}(x, \bar{y}, \bar{z}=0). \quad (75)$$

By equations (74) and (75) we obtain for the downwash in the wing-body junction, $|y| = R$, the value

$$\frac{v_z(x, |y|=R, z=0)}{V_0} = \frac{A}{2\pi}\tan\varphi\left\{\lim_{\bar{y}\to 0}\frac{\bar{y}}{\bar{s}}-\log\frac{\sqrt{(\bar{s}^2+4R^2)}+\bar{s}}{2R}\right\}. \quad (76)$$

This has the same singular behaviour as at the centre section of an isolated wing. We note that for $R = 0$, i.e., $\bar{y} = y$, $\bar{s} = s = x/\tan\varphi$, the value of v_z by equations (74) and (75) agrees with that of equation (66), as is necessary because for $M_0 = 1$ linear theory and slender-body theory give the same results. Introducing the spanwise ordinate $y^* = y - R$, we obtain for the limit $R \to \infty : \bar{y} = 2y^*$ and by equations (74) and (75)

$$\frac{v_z(x, y^*, o)}{V_0} = \frac{A}{4\pi}\tan\varphi\log\frac{y^{*2}}{s^{*2}-y^{*2}}$$

$$=-\frac{A}{4\pi}\tan\varphi\log\frac{x^2-y^{*2}\tan^2\varphi}{y^{*2}\tan^2\varphi},$$

which also agrees with equation (66).

This result is comparable to the fact that the distribution of the streamwise velocity component v_x at the junction of a cylindrical fuselage and a swept wing with symmetrical section, both at zero incidence, is similar to that at the centre section of the corresponding isolated wing. This theoretical result has been confirmed by experiments. The body acts in both cases like a reflection plate.

It has sometimes been argued that, when determining the shape of the aerofoil section at the junction of a fuselage and a wing with constant spanwise load distribution, one need not take account of the singular behaviour of the downwash in the plane $z = 0$, since the stations near the centre of the isolated wing are buried within the fuselage. Equation (76) shows that this reasoning is fallacious. As a first approximation to the camber and twist required in and near the junction we may take the wing shape at and near the centre of the isolated wing.

9. *Wings Without the Singular Behaviour of the Downwash at the Centre Section.*—The question arises whether the singular behaviour of the downwash at the centre section of the chordal plane cannot be avoided. For a wing with a discontinuity in the leading edge, this is only possible by relaxing the condition of constant spanwise load distribution.

To obtain the full benefit of a swept plan-form the isobar pattern must have a minimum sweep over the whole wing. This condition can be satisfied by an isobar pattern with varying sweep, provided that, near the centre section, the isobars are more highly swept than further out on the wing. Such an isobar pattern may be obtained by a suitable choice of the load distribution.

For the centre portion of the wing the load distribution could be similar to that on a plane delta wing at incidence or to that on a delta wing with conical flow, cambered and twisted so as to have no singular behaviour of the downwash in the wing plane. Due to the conical conditions the isobars of such a wing all run into the apex. This may cause rather sudden changes of the pressure at stations somewhat away from the centre section. The adverse pressure gradients are probably so high that the real viscous flow is likely to separate near the apex, so that such a design does not seem to be desirable.

More favourable pressure gradients can be obtained with a load distribution such that the various isobars end at different spanwise positions at the leading edge. However, this implies zero load at the centre section of the wing. Such a design has the disadvantage that for a given total lift coefficient the outer wing has to be more highly loaded than for a constant $C_L(y)$ design ; this requires a thinner or more highly swept wing for a given critical Mach number. Furthermore, the vortex drag of a wing with zero load at the centre section is very much larger than for a wing with constant $C_L(y)$.

10. *Concluding Summary.*—The mean surface of a swept wing with constant chordwise load distribution along the span cannot be calculated by applying the ordinary linear theory, due to a singular behaviour of the downwash at the centre section. This difficulty can be overcome by applying the approximate procedure of calculating the downwash induced by a plane sheet of doublets at a finite distance equal to the wing thickness. Explicit formulae for the downwash in supersonic, sonic and incompressible flow have been worked out for linearly varying load distributions. The differences in the mean surfaces for low supersonic and sonic main flow are relatively small, so that the effect of varying the load distribution can be studied for the much simpler case of sonic main flow. The section shape, determined for sonic main flow, requires a rather rapid decrease of the twist and a noticeable variation of the camber-line across the span. The sections calculated for the centre of a swept-back wing can also be used as an approximation to the section shape at the junction of the wing with a body. A few load distributions have been considered which vary in such a way along the span that they produce a regular behaviour of the downwash at the centre section. However, the corresponding wings have some undesirable properties, such as large adverse pressure gradients or large vortex drag. Therefore, it seems worthwhile to investigate experimentally the properties of a wing with constant spanwise load distribution designed according to the suggested procedure.

LIST OF SYMBOLS

x, y, z — Rectangular co-ordinates, x axis along the centre-section chord, y spanwise z positive upwards

$\xi = x - |y| \tan \varphi$

$\zeta = y + iz$, complex co-ordinate

$\bar{\zeta} = \bar{y} + i\bar{z}$, co-ordinate in transformed plane

x_1		*See* equation (7) and Fig. 1
$z(x)$		Aerofoil-section ordinate
$z_t(x)$	=	$\frac{1}{2}(z_U(x) - z_L(x))$, ordinate of thickness distribution
$z_c(x)$	=	$\frac{1}{2}(z_U(x) + z_L(x))$, ordinate of camber-line
c		Wing chord
t		Wing thickness
s	=	$s(x)$, local wing span
$\bar{s}$		Span in transformed plane
R		Body radius
α_τ		Angle of twist
φ		Angle of sweep
V_0		Velocity of main stream
V_{x0}, V_{z0}		Component of V_0 in direction of the axes
v_x, v_z		Velocity increments in direction of the axes
M_0		Mach number of the free stream
β	=	$\sqrt{(\lvert M_0^2 - 1\rvert)}$
ϕ		Velocity potential
$\Delta\phi$	=	$\phi_U - \phi_L$
C_p		Pressure coefficient
$l(x, y)$	=	$-\{C_{pU}(x, y) - C_{pL}(x, y)\}$, load coefficient
$C_L(y)$		Local lift coefficient
Γ		Circulation
γ		Strength of vortex distribution
$C_D(y)$		Sectional drag coefficient
A, B		*See* equations (8), (9) and (26)
σ		*See* equation (56)
σ^*		*See* equation (60)
J_1, J_2		Integrals (*see* equations (11) and (12) and the Appendix)
J_3, J_4, J_5		Integrals (*see* equation (35))

Suffices :

U	Upper surface
L	Lower surface

REFERENCES

No.	Author	Title, etc.
1	A. Robinson and J. A. Laurmann ..	*Wing Theory.* Cambridge University Press. 1956.
2	D. Küchemann and J. Weber	*Aerodynamics of Propulsion.* McGraw-Hill Book Company. 1953.
3	J. Weber	The calculation of the pressure distribution on the surface of thick cambered wings and the design of wings with given pressure distribution. R. & M. 3026. June, 1955.
4	D. Küchemann	A simple method for calculating the span and chordwise loadings on thin swept wings. (Unpublished M.O.S. Report.)
5	D. Küchemann and J. Weber	On the chordwise lift distribution at the centre of swept wings. *Aero. Quart.* Vol. II. p. 146. 1950.
6	D. Küchemann	The distribution of lift over the surface of swept wings. *Aero. Quart.* Vol. IV. p. 261. 1953.
7	D. Küchemann	A simple method for calculating the span and chordwise loading on straight and swept wings of any given aspect ratio at subsonic speeds. R. & M. 2935. August, 1952.
8	D. Küchemann, J. Weber and G. G. Brebner	Low speed tests on wings of 45-deg sweep. Part II : Balance and pressure measurements on wings of different aspect ratios. R. & M. 2882. May, 1951.

APPENDIX

Explicit expressions are required for the following two integrals :

$$J_1 = \int_0^{x_1} \frac{dx'}{(x'^2 + z^2 \tan^2\varphi)\sqrt{[\tan^2\varphi\{(x-x')^2 - \beta^2 z^2\} - \beta^2 x'^2]}}$$

$$J_2 = \int_0^{x_1} \frac{x'\,dx'}{(x'^2 + z^2 \tan^2\varphi)\sqrt{[\tan^2\varphi\{(x-x')^2 - \beta^2 z^2\} - \beta^2 x'^2]}}.$$

With the notation :

$$A = \frac{x \tan^2\varphi}{\tan^2\varphi - \beta^2}$$

$$B = \frac{\beta \tan\varphi}{\tan^2\varphi - \beta^2}\sqrt{\{x^2 + z^2(\tan^2\varphi - \beta^2)\}}$$

and introducing the transformations :

$$x' - A = B\cosh u$$

$$t = \tanh\frac{u}{2}$$

and using the value of x_1 given by equation (7), the integral J_1 can be written as :

$$J_1 = \frac{-2}{\sqrt{(\tan^2\varphi - \beta^2)}} \int_{t_0}^{\infty} \frac{-t^2 + 1}{\gamma t^4 - 2\delta t^2 + \varepsilon}\,dt$$

with

$$\gamma = (A - B)^2 + z^2 \tan^2 \varphi$$
$$\delta = A^2 - B^2 + z^2 \tan^2 \varphi$$
$$\varepsilon = (A + B)^2 + z^2 \tan^2 \varphi$$
$$t_0^2 = \frac{A + B}{A - B}.$$

By partial fractions :

$$J_1 = \frac{-2}{\sqrt{(\tan^2 \varphi - \beta^2)}} \int_{t_0}^{\infty} \left(\frac{a_3 t + a_4}{\gamma t^2 + a_1 t + a_2} + \frac{-a_3 t + a_4}{\gamma t^2 - a_1 t + a_2} \right) dt$$

$$= \frac{-2}{\sqrt{(\tan^2 \varphi - \beta^2)}} \left\{ \frac{\gamma + a_2}{4 a_1 a_2} \log \frac{\gamma t_0^2 - a_1 t_0 + a_2}{\gamma t_0^2 + a_1 t_0 + a_2} \right.$$

$$\left. + \frac{\gamma - a_2}{2 a_2 \sqrt{(4 a_2 \gamma - a_1^2)}} \tan^{-1} \frac{t_0 \sqrt{(4 a_2 \gamma - a_1^2)}}{\gamma t_0^2 - a_2} \right\}$$

with

$$a_1 = -\sqrt{[2\gamma\{\delta + \sqrt{(\varepsilon\gamma)}\}]}$$
$$a_2 = \sqrt{(\varepsilon\gamma)}$$
$$a_3 = \frac{\gamma^2}{2 a_1 a_2} + \frac{\gamma}{2 a_1}$$
$$a_4 = \frac{\gamma}{2 a_2}.$$

In a similar way, we obtain :

$$J_2 = \frac{-2}{\sqrt{(\tan^2 \varphi - \beta^2)}} \int_{t_0}^{\infty} \frac{\varkappa t^2 + \lambda}{\gamma t^4 - 2\delta t^2 + \varepsilon} dt$$

$$= \frac{-2}{\sqrt{(\tan^2 \varphi - \beta^2)}} \left\{ \frac{a_5}{2\gamma} \log \frac{\gamma t_0^2 - a_1 t_0 + a_2}{\gamma t_0^2 + a_1 t_0 + a_2} \right.$$

$$\left. + \frac{2 a_6 \gamma - a_1 a_5}{\gamma \sqrt{(4 a_2 \gamma - a_1^2)}} \tan^{-1} \frac{t_0 \sqrt{(4 a_2 \gamma - a_1^2)}}{\gamma t_0^2 - a_2} \right\}$$

with

$$\varkappa = -(A - B)$$
$$\lambda = A + B$$
$$a_5 = \frac{\lambda \gamma^2}{2 a_1 a_2} - \frac{\varkappa \gamma}{2 a_1}$$
$$a_6 = \frac{\lambda \gamma}{2 a_2}.$$

Since in practice $z \ll x$ for most of the wing, it is advisable to express the integrals J_1 and J_2 as power series in z. This leads to the result :

$$J_1 = \frac{\pi/2}{xz \tan^2 \varphi} - \tan \varphi \log \frac{|z| \beta}{2x}$$

$$- \frac{\sqrt{(\tan^2 \varphi - \beta^2)}}{\tan \varphi} + \text{terms of order } z$$

$$J_2 = - \frac{1}{x \tan \varphi} \log \frac{|z|\beta}{2x} - \frac{z}{x^2} \frac{\pi}{2}$$

$$+ \text{terms of order } z^2.$$

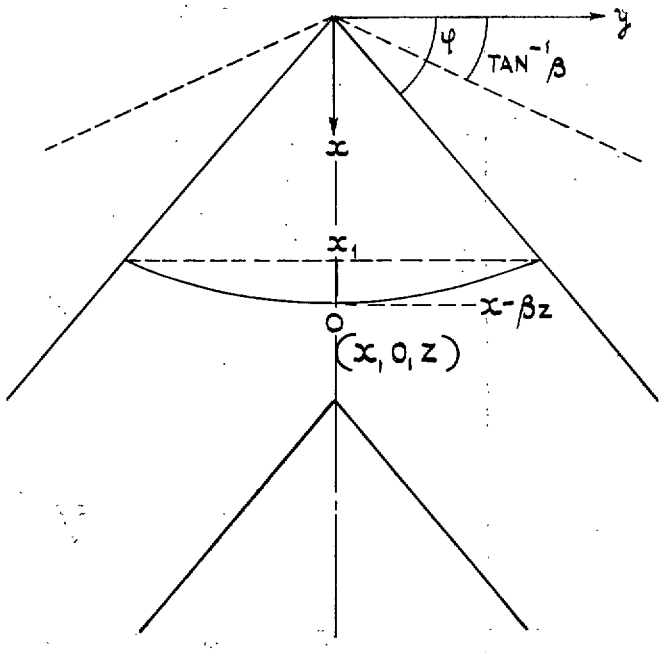

FIG. 1. Notation.

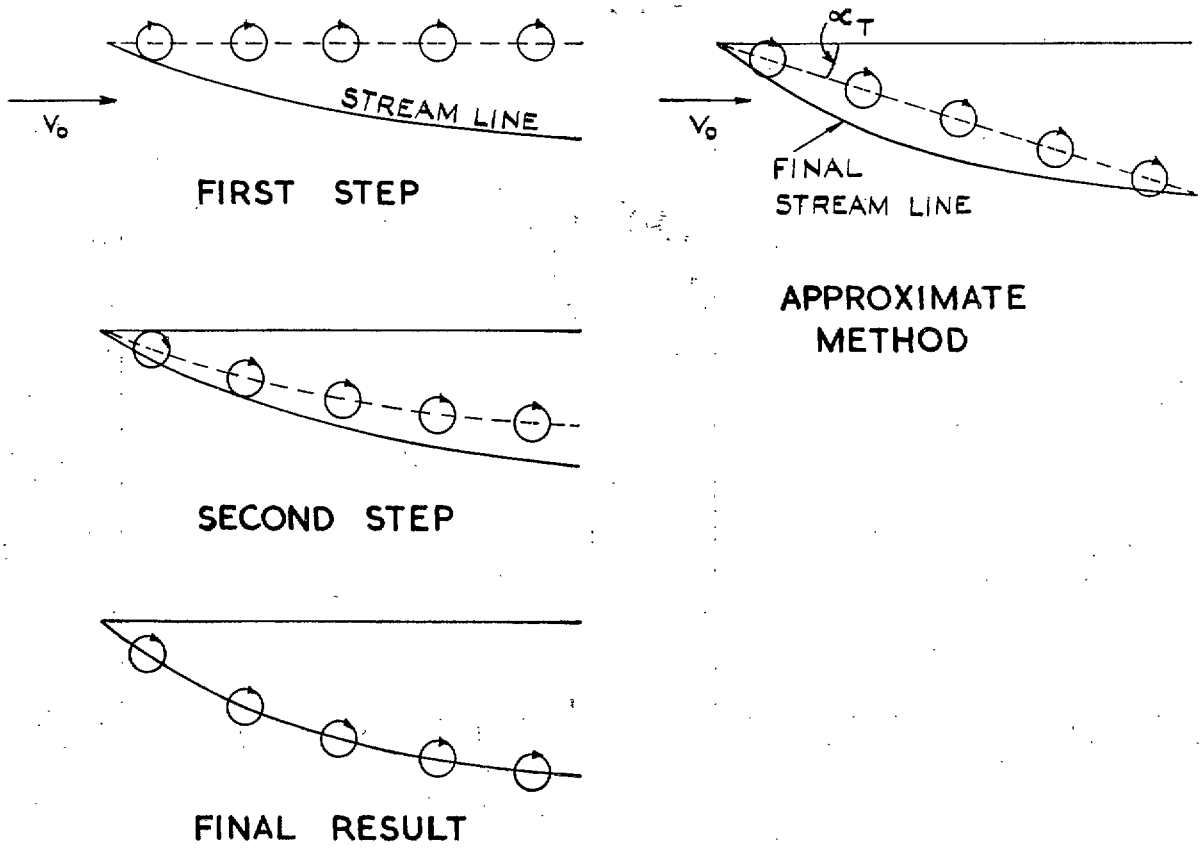

FIG. 2. Sketch of an iteration procedure for determining the aerofoil surface and of an approximate method.

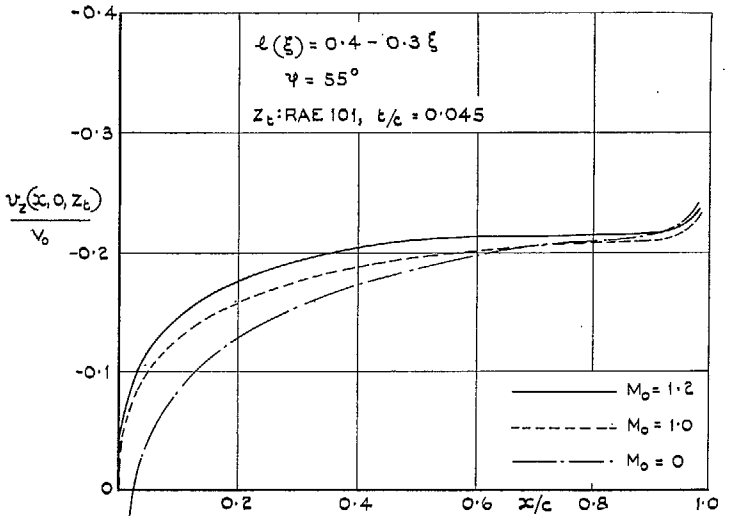

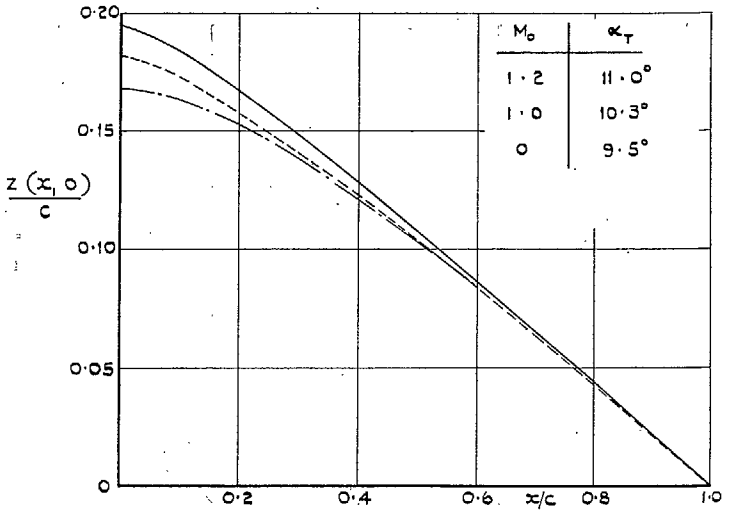

FIG. 3. Downwash distributions and section shapes at the centre section of swept-back wings of infinite span with constant spanwise load distribution for various Mach numbers.

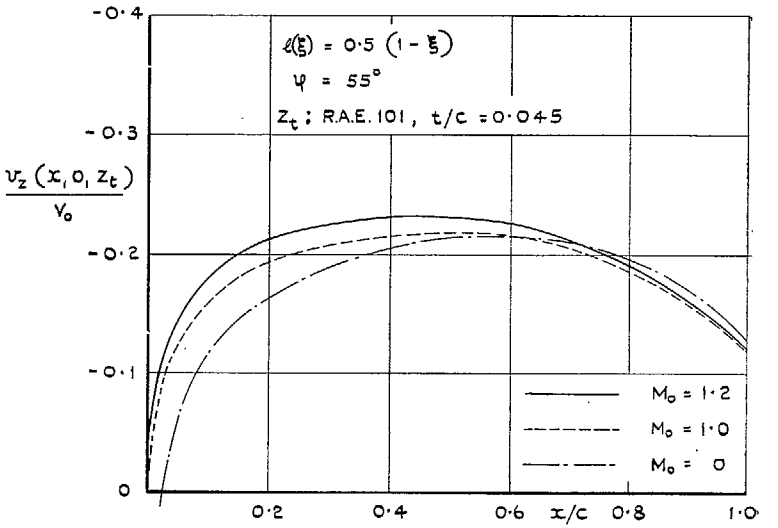

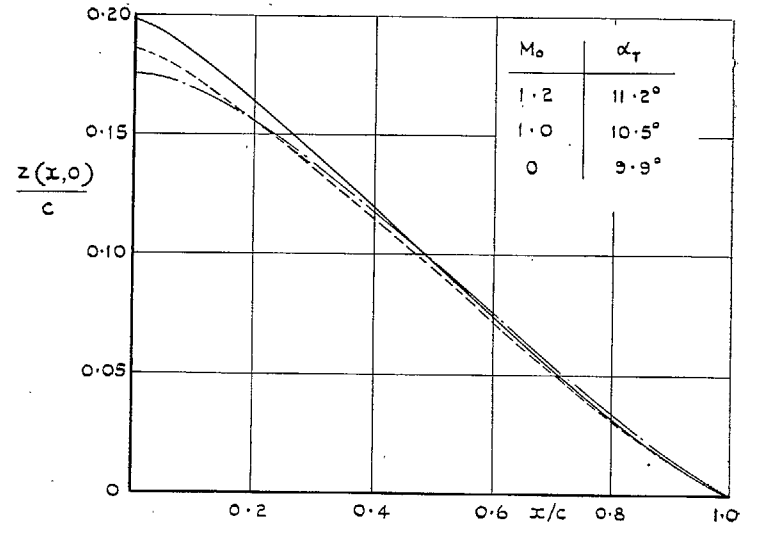

FIG. 4. Downwash distributions and section shapes at the centre section of swept-back wings of infinite span with constant spanwise load distribution for various Mach numbers.

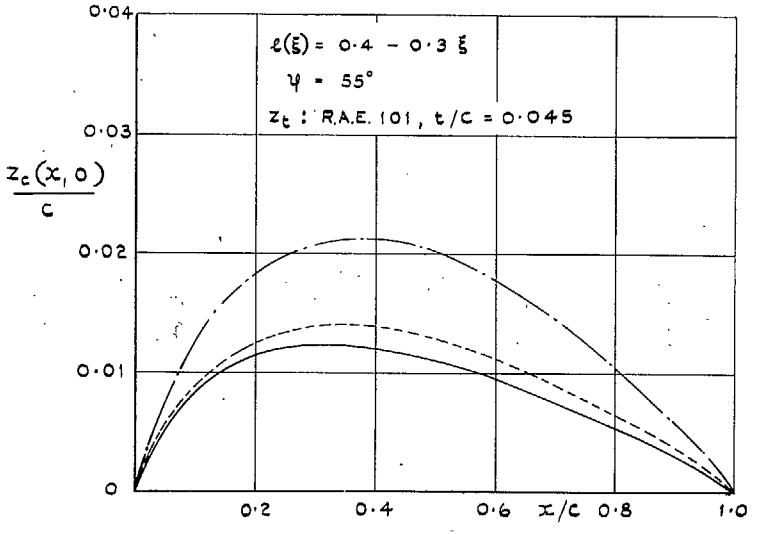

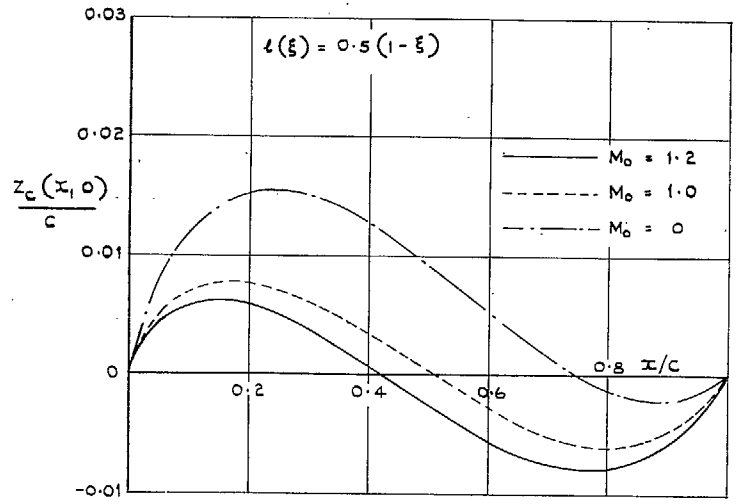

FIG. 5. Camber-lines at the centre section of swept-back wings of infinite span with constant spanwise load distribution for various Mach numbers.

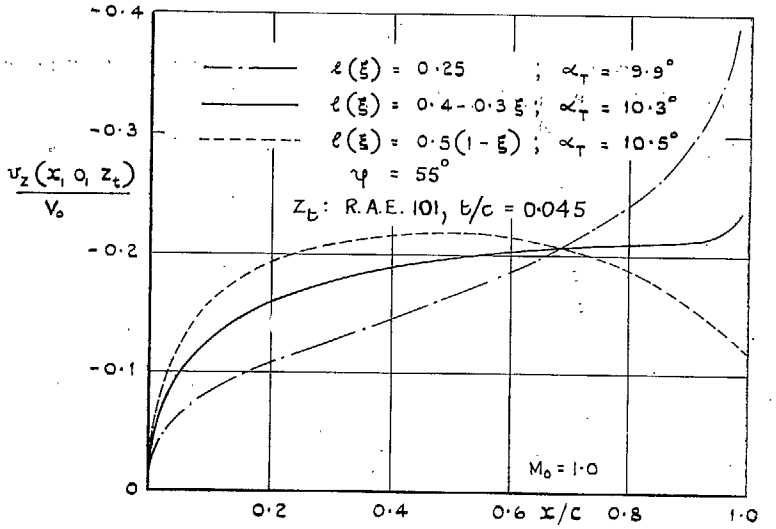

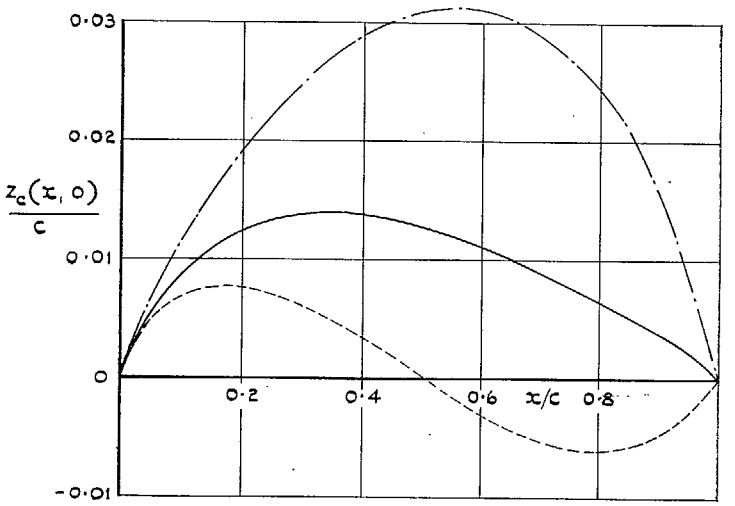

FIG. 6. Downwash distributions and camber-lines at the centre section of swept-back wings with constant spanwise load distribution for various chordwise load distributions.

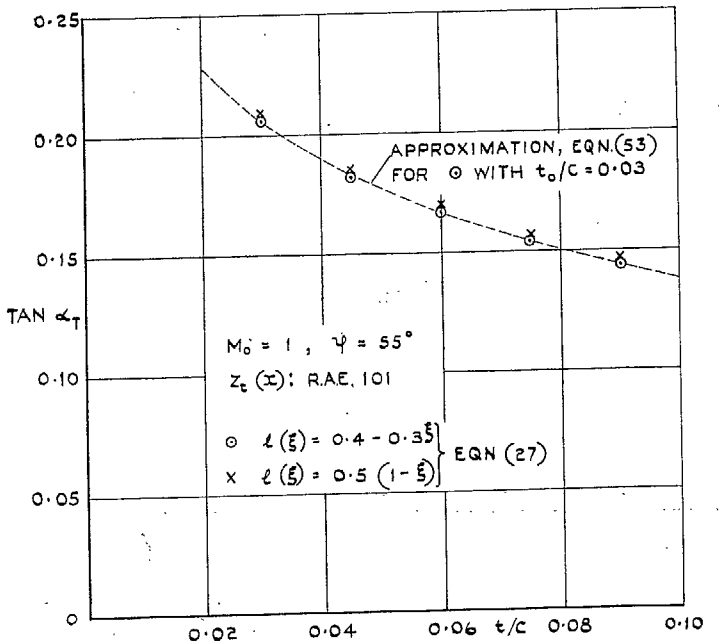

FIG. 7. Variation with thickness/chord ratio of the twist at the centre section of swept-back wings with constant spanwise load distribution.

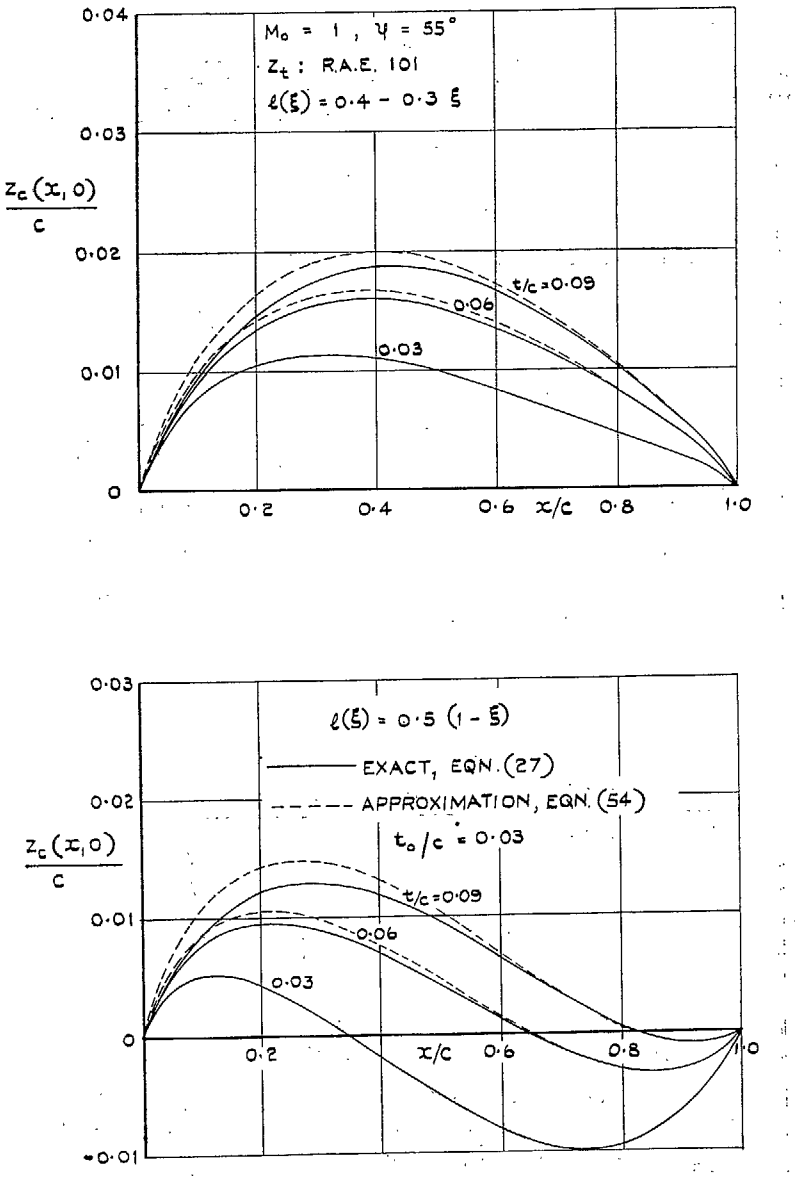

FIG. 8. Variation with thickness/chord ratio of the camber-lines at the centre section of swept-back wings with constant spanwise load distribution.

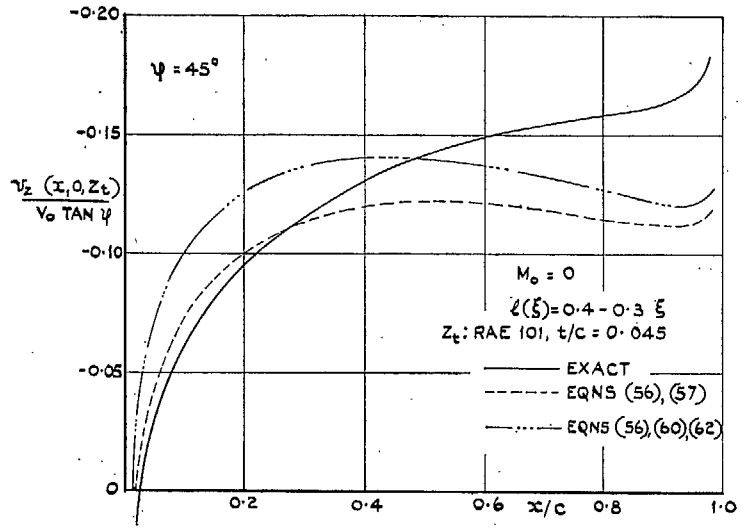

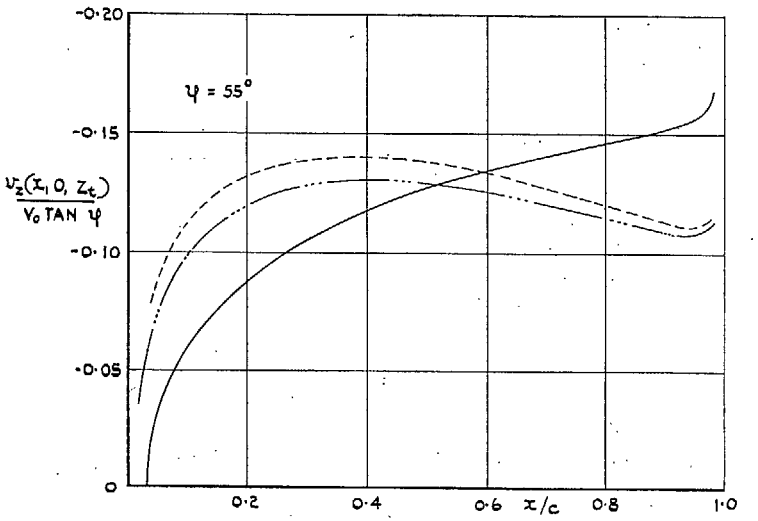

FIG. 9a. Various approximations to the downwash distribution at the centre section of swept-back wings of infinite span with constant spanwise load distributions.

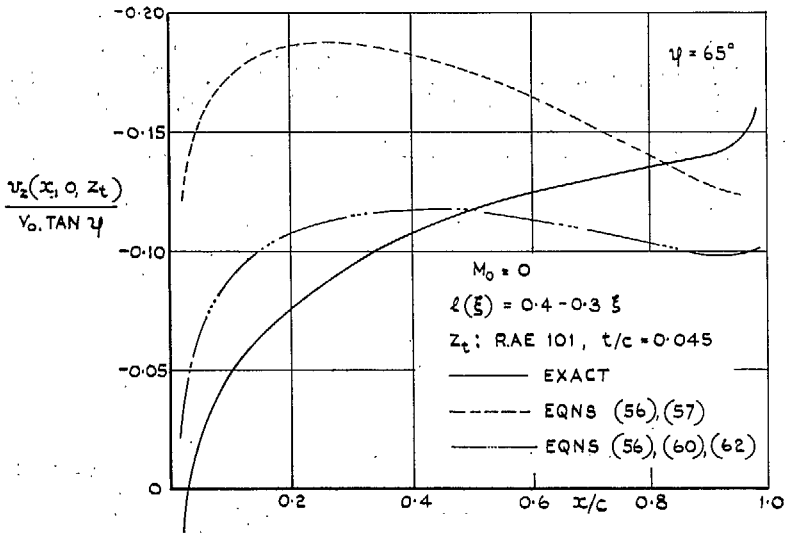

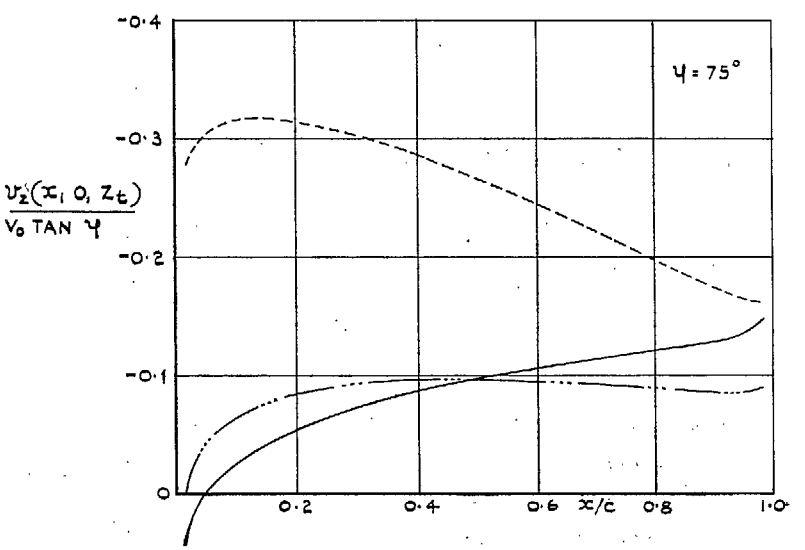

FIG. 9b. Various approximations to the downwash distribution at the centre section of swept-back wings of infinite span with constant spanwise load distributions.

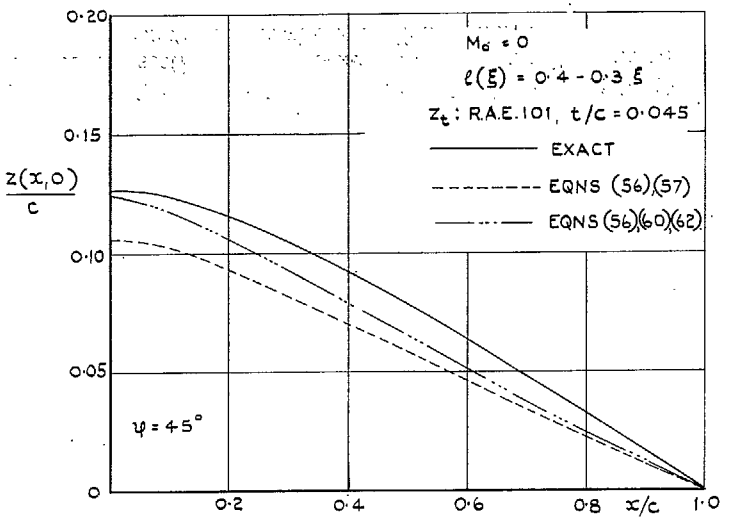

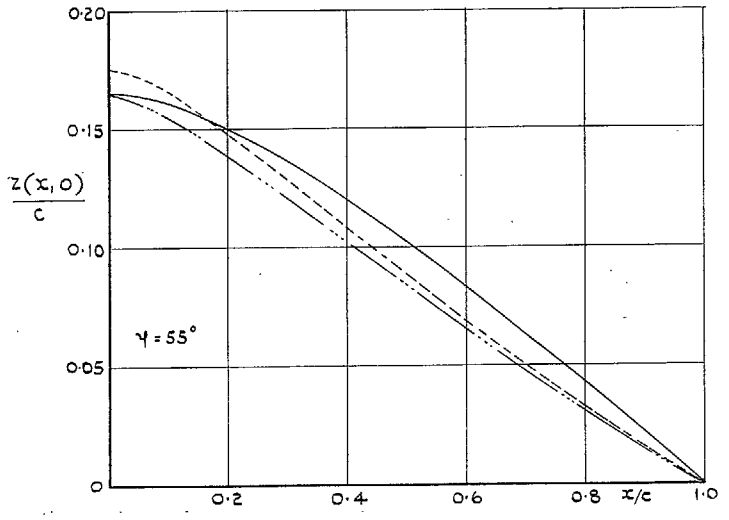

FIG. 10a. Section shapes at the centre section of swept-back wings of infinite span with constant spanwise load distribution obtained from various approximations to the downwash distribution.

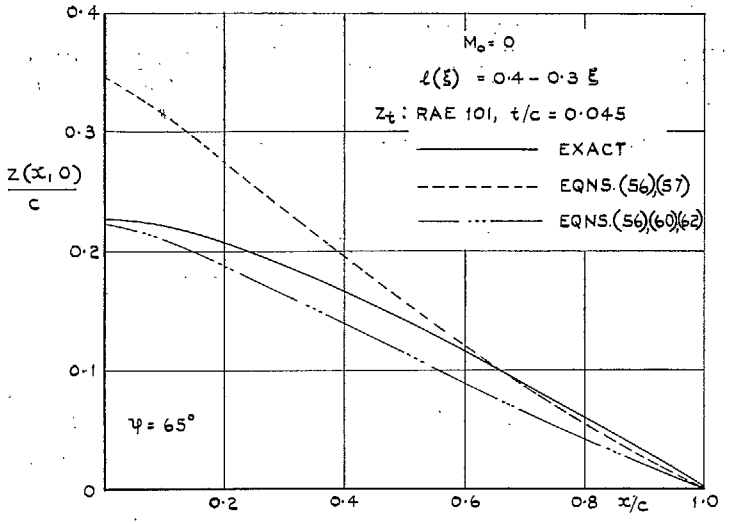

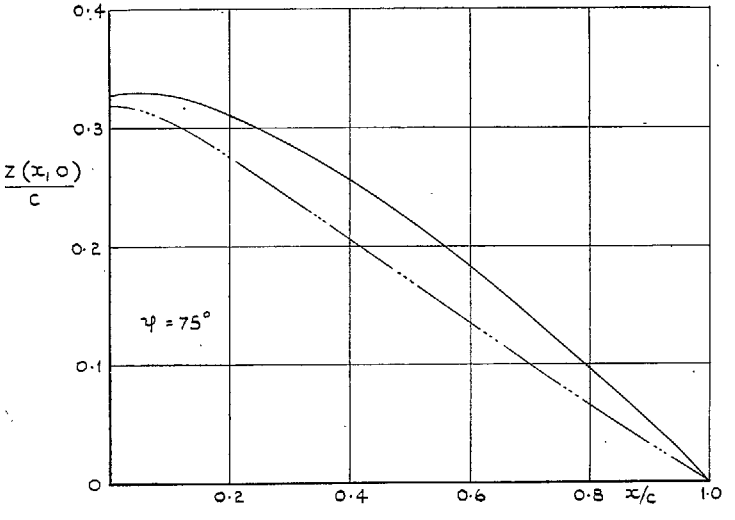

FIG. 10b. Section shapes at the centre section of swept-back wings of infinite span with constant spanwise load distribution obtained from various approximations to the downwash distribution.

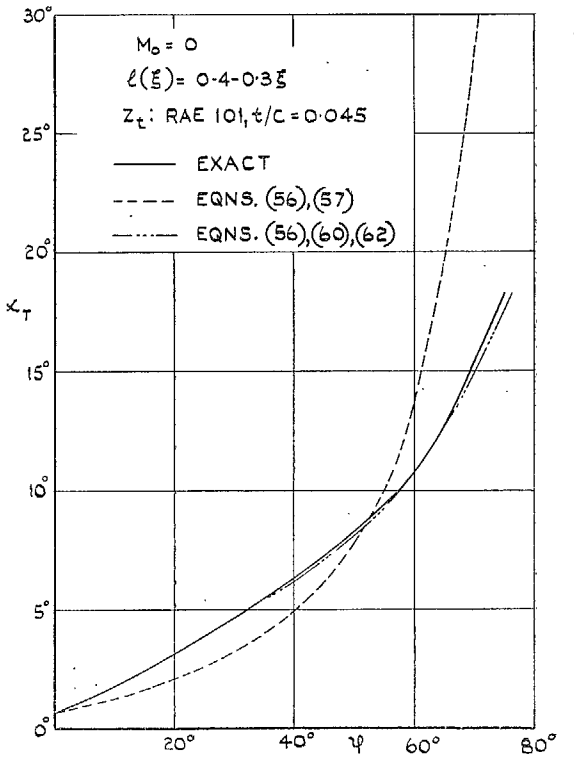

FIG. 11. Variation with angle of sweep of the twist at the centre section of swept-back wings of infinite span with constant spanwise load distribution.

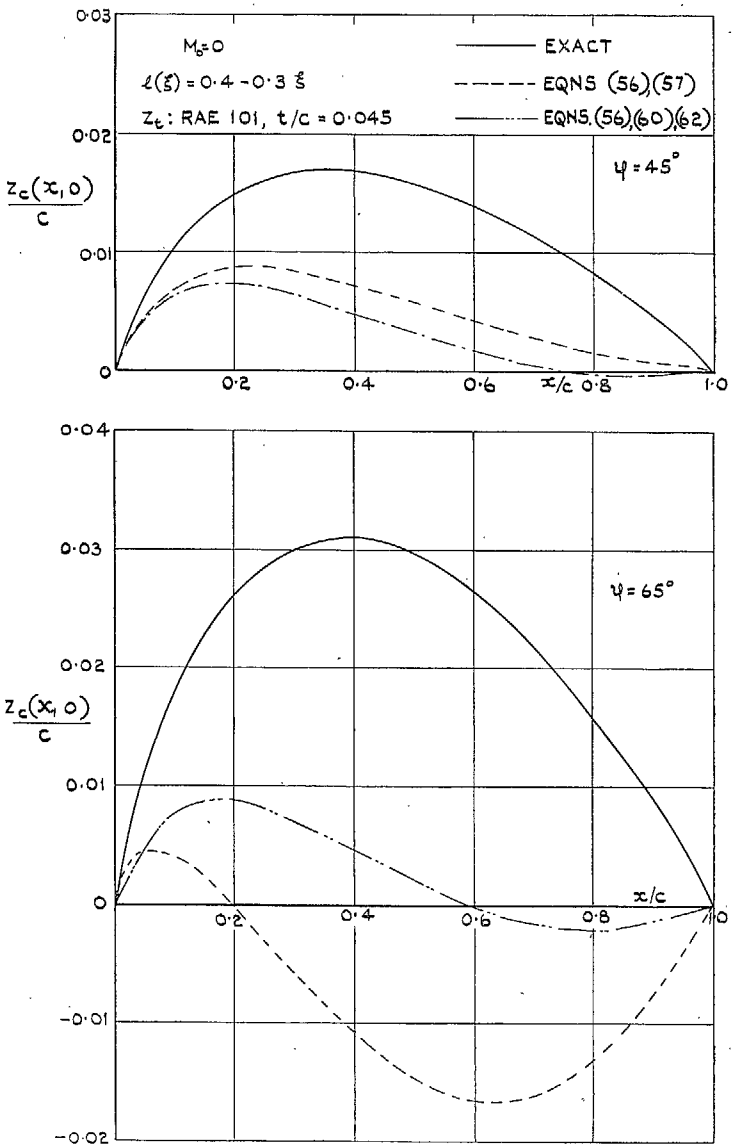

FIG. 12. Camber-lines at the centre section of swept-back wings of infinite span with constant spanwise load distribution obtained from various approximations to the downwash distribution.

J4393 Wt.53/2293 K7 7/58 D&Co. 34/263

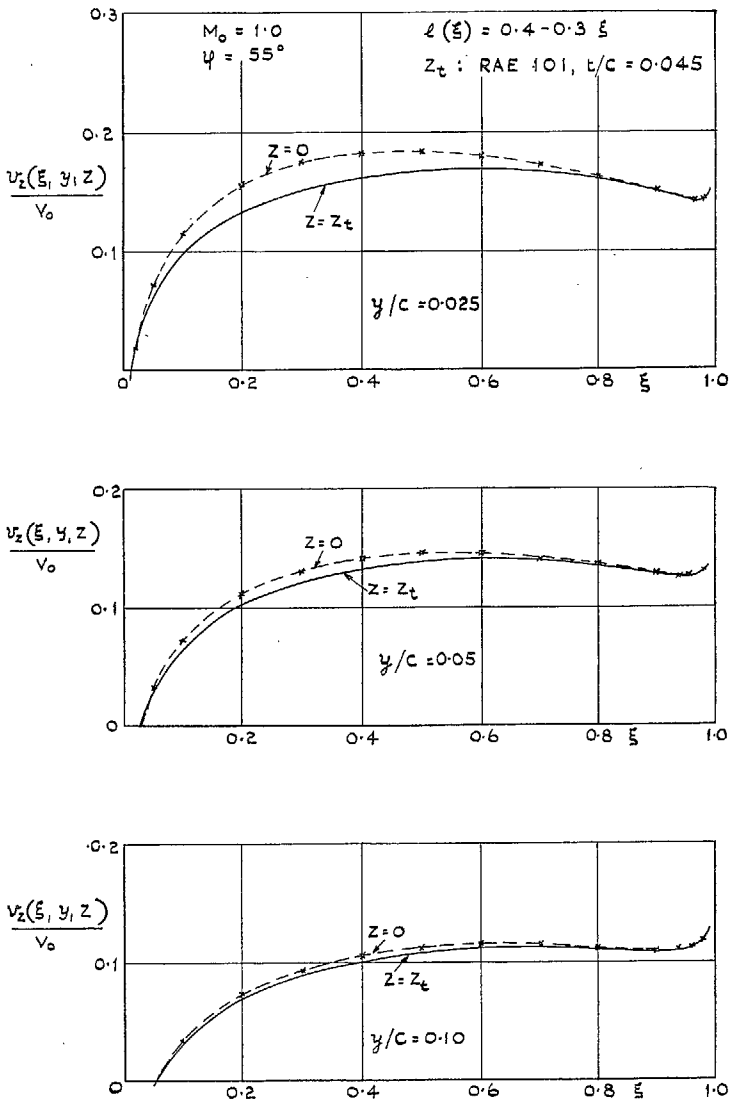

FIG. 13. Downwash distributions at various spanwise stations near the centre of a swept-back wing of infinite span with constant spanwise load distribution.

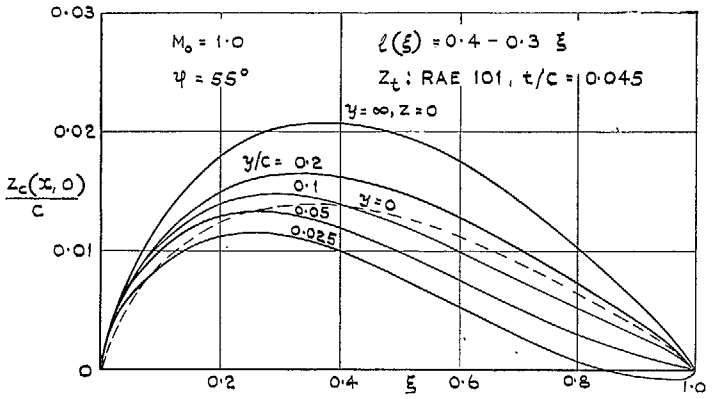

FIG. 14. Camber-lines for various spanwise stations of a swept-back wing of infinite span with constant spanwise load distribution.

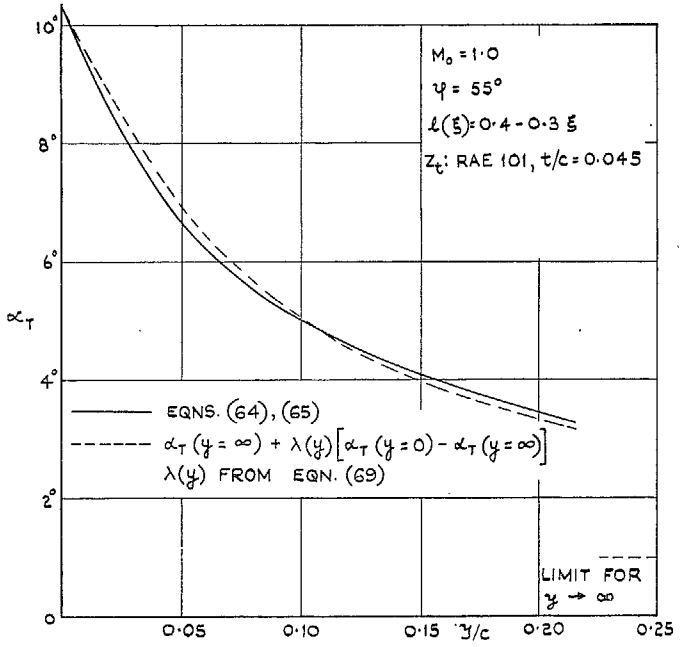

FIG. 15. Spanwise variation of the twist on a swept-back wing of infinite span with constant spanwise load distribution.

PRINTED IN GREAT BRITAIN

Publications of the Aeronautical Research Council

ANNUAL TECHNICAL REPORTS OF THE AERONAUTICAL RESEARCH COUNCIL (BOUND VOLUMES)

1939 Vol. I. Aerodynamics General, Performance, Airscrews, Engines. 50*s.* (52*s.*)

Vol. II. Stability and Control, Flutter and Vibration, Instruments, Structures, Seaplanes, etc. 63*s.* (65*s.*)

1940 Aero and Hydrodynamics, Aerofoils, Airscrews, Engines, Flutter, Icing, Stability and Control, Structures, and a miscellaneous section. 50*s.* (52*s.*)

1941 Aero and Hydrodynamics, Aerofoils, Airscrews, Engines, Flutter, Stability and Control, Structures. 63*s.* (65*s.*)

1942 Vol. I. Aero and Hydrodynamics, Aerofoils, Airscrews, Engines. 75*s.* (77*s.*)

Vol. II. Noise, Parachutes, Stability and Control, Structures, Vibration, Wind Tunnels. 47*s.* 6*d.* (49*s.* 6*d.*)

1943 Vol. I. Aerodynamics, Aerofoils, Airscrews. 80*s.* (82*s.*)

Vol. II. Engines, Flutter, Materials, Parachutes, Performance, Stability and Control, Structures. 90*s.* (92*s.* 9*d.*)

1944 Vol. I. Aero and Hydrodynamics, Aerofoils, Aircraft, Airscrews, Controls. 84*s.* (86*s.* 6*d.*)

Vol. II. Flutter and Vibration, Materials, Miscellaneous, Navigation, Parachutes, Performance, Plates and Panels, Stability, Structures, Test Equipment, Wind Tunnels. 84*s.* (86*s.* 6*d.*)

1945 Vol. I. Aero and Hydrodynamics, Aerofoils. 130*s.* (132*s.* 9*d.*)

Vol. II. Aircraft, Airscrews, Controls. 130*s.* (132*s.* 9*d.*)

Vol. III. Flutter and Vibration, Instruments, Miscellaneous, Parachutes, Plates and Panels, Propulsion. 130*s* (132*s.* 6*d.*)

Vol. IV. Stability, Structures, Wind tunnels, Wind Tunnel Technique. 130*s.* (132*s.* 6*d.*)

ANNUAL REPORTS OF THE AERONAUTICAL RESEARCH COUNCIL—

1937 2*s.* (2*s.* 2*d.*) 1938 1*s.* 6*d.* (1*s.* 8*d.*) 1939–48 3*s.* (3*s.* 5*d.*)

INDEX TO ALL REPORTS AND MEMORANDA PUBLISHED IN THE ANNUAL TECHNICAL REPORTS, AND SEPARATELY—

April, 1950 – – – – – R. & M. No. 2600. 2*s.* 6*d.* (2*s.* 10*d.*)

AUTHOR INDEX TO ALL REPORTS AND MEMORANDA OF THE AERONAUTICAL RESEARCH COUNCIL—

1909–January, 1954 – – – R. & M. No. 2570. 15*s.* (15*s.* 8*d.*)

INDEXES TO THE TECHNICAL REPORTS OF THE AERONAUTICAL RESEARCH COUNCIL—

December 1, 1936 — June 30, 1939. R. & M. No. 1850. 1*s.* 3*d.* (1*s.* 5*d.*)

July 1, 1939 — June 30, 1945. – R. & M. No. 1950. 1*s.* (1*s.* 2*d.*)

July 1, 1945 — June 30, 1946. – R. & M. No. 2050. 1*s.* (1*s.* 2*d.*)

July 1, 1946 — December 31, 1946. R. & M. No. 2150. 1*s.* 3*d.* (1*s.* 5*d.*)

January 1, 1947 — June 30, 1947. – R. & M. No. 2250. 1*s.* 3*d.* (1*s.* 5*d.*)

PUBLISHED REPORTS AND MEMORANDA OF THE AERONAUTICAL RESEARCH COUNCIL—

Between Nos. 2251–2349. – – R. & M. No. 2350. 1*s.* 9*d.* (1*s.* 11*d.*)

Between Nos. 2351–2449. – – R. & M. No. 2450. 2*s.* (2*s.* 2*d.*)

Between Nos. 2451–2549. – – R. & M. No. 2550. 2*s.* 6*d.* (2*s.* 10*d.*)

Between Nos. 2551–2649. – – R. & M. No. 2650. 2*s.* 6*d.* (2*s.* 10*d.*)

Between Nos. 2651–2749. – – R. & M. No. 5750. 2*s.* 6*d.* (2*s.* 10*d.*)

Prices in brackets include postage

HER MAJESTY'S STATIONERY OFFICE

York House, Kingsway, London W.C.2; 423 Oxford Street, London W.1;
13a Castle Street, Edinburgh 2; 39 King Street, Manchester 2; 2 Edmund Street, Birmingham 3; 109 St. Mary Street, Cardiff; Tower Lane, Bristol 1; 80 Chichester Street, Belfast, *or through any bookseller*

S.O. Code No. 23-3098